Characteristics of $PM_{2.5}$ mass concentrations and chemical species in urban and background areas of China: emerging results from the CARE-China network

Zirui Liu[1*], Wenkang Gao[1], Yangchun Yu[1], Bo Hu[1], Jinyuan Xin[1], Yang Sun[1], Lili Wang[1], Gehui Wang[3], Xinhui Bi[4], Guohua Zhang[4], Honghui Xu[5], Zhiyuan Cong[6], Jun He[7], Jingsha Xu[7], Yuesi Wang[1,2*]

[1]State Key Laboratory of Atmospheric Boundary Layer Physics and Atmospheric Chemistry, Institute of Atmospheric Physics, Chinese Academy of Sciences, Beijing 100029, China

[2]Center for Excellence in Regional Atmospheric Environment, Institute of Urban Environment, Chinese Academy of Sciences, Xiamen 361021, China

[3]State Key Laboratory of Loess and Quaternary Geology, Institute of Earth Environment, Chinese Academy of Sciences, Xi'an 710075, China

[4]State Key Laboratory of Organic Geochemistry, Guangzhou Institute of Geochemistry, Chinese Academy of Sciences, Guangzhou 510640, China

[5]Zhejiang Meteorology Science Institute, Hangzhou 310017, China

[6]Key Laboratory of Tibetan Environment Changes and Land Surface Processes, Institute of Tibetan Plateau Research, Chinese Academy of Sciences, Beijing 100101, China

[7]International Doctoral Innovation Centre, The University of Nottingham Ningbo China, Ningbo 315100, China

[*]Corresponding author: Z.R Liu (Liuzirui@mail.iap.ac.cn); Y.S Wang (wys@mail.iap.ac.cn)

Abstract: The "Campaign on atmospheric Aerosol REsearch" network of China (CARE-China) is a long-term project for the study of the spatiotemporal distributions of physical aerosol characteristics as well as the chemical components and optical properties of aerosols over China. This study presents the first long-term datasets from this project, including three years of observations of online $PM_{2.5}$ mass concentrations (2012-2014) and one year of observations of $PM_{2.5}$ compositions (2012-2013) from the CARE-China network. The average $PM_{2.5}$ concentrations at 20 urban sites is 73.2 μg/m^3 (16.8-126.9 μg/m^3), which was three times higher than the average value from the 12 background sites (11.2-46.5 μg/m^3). The $PM_{2.5}$ concentrations are generally higher in east-central China than in the other parts of the country due to their relative large particulate matter (PM) emissions and the unfavorable meteorological conditions for pollution dispersion. A distinct seasonal variability of the $PM_{2.5}$ is observed, with highs in the winter and lows during the summer at urban sites. Inconsistent seasonal trends were observed at the background sites. Bimodal and unimodal diurnal variation patterns were identified at both urban and background sites. The chemical compositions of $PM_{2.5}$ at six paired urban and background sites located within the most polluted urban agglomerations (North China Plain (NCP), Yangtze River Delta (YRD), Pearl River Delta (PRD), Northeast China Region (NECR), Southwestern China Region (SWCR)) and cleanest regions (Tibetan Autonomous Region (TAR)) of China were analyzed. The major $PM_{2.5}$ constituents across all the urban sites are organic matter (OM, 26.0%), SO_4^{2-}(17.7%), mineral dust (11.8%), NO_3^- (9.8%), NH_4^+ (6.6%), elemental carbon (EC) (6.0%), Cl^- (1.2%) at 45% RH and unaccounted matter (20.7%). Similar chemical compositions of $PM_{2.5}$ were observed at background sites but were associated with higher fractions of OM (33.2%) and lower fractions of NO_3^- (8.6%) and EC (4.1%). Significant variations of the chemical species were observed among the sites. At the urban sites, the OM ranged from 12.6 μg/m^3 (Lhasa) to 23.3 μg/m^3 (Shenyang), the SO_4^{2-} ranged from 0.8 μg/m^3

(Lhasa) to 19.7 μg/m^3 (Chongqing), the NO_3^- ranged from 0.5 μg/m^3 (Lhasa) to 11.9 μg/m^3 (Shanghai) and the EC ranged from 1.4 μg/m^3 (Lhasa) to 7.1 μg/m^3 (Guangzhou). The $PM_{2.5}$ chemical species at the background sites exhibited larger spatial heterogeneities than those at urban sites, suggesting the different contributions from regional anthropogenic or natural emissions and from the long-range transport to background areas. Notable seasonal variations of $PM_{2.5}$ polluted days were observed, especially for the megacities in east-central China, resulting in frequent heavy pollution episodes occurring during the winter. The evolution of the $PM_{2.5}$ chemical compositions on polluted days was consistent for the urban and nearby background sites, where the sum of sulfate, nitrate and ammonia typically constituted much higher fractions (31-57%) of $PM_{2.5}$ mass, suggesting fine particle pollution in the most polluted areas of China assumes a regional tendency, and the importance to address the emission reduction of secondary aerosol precursors including SO_2 and NOx. Furthermore, distinct differences in the evolution of $[NO_3^-]/[SO_4^{2-}]$ ratio and OC/EC ratio in polluted days imply that mobile sources and stationary (coal combustion) sources are likely more important in Guangzhou and Shenyang, respectively, whereas in Beijing it is mobile emission and residential sources. As for Chongqing, the higher oxidation capacity than the other three cities suggested it should pay more attention to the emission reduction of secondary aerosol precursors. This analysis reveals the spatial and seasonal variabilities of the urban and background aerosol concentrations on a national scale and provides insights into their sources, processes, and lifetimes.

1. Introduction

Atmospheric fine particulate matter ($PM_{2.5}$) is a complex heterogeneous mixture, whose physical size distribution and chemical composition change in time and space and are dependent on the emission sources, atmospheric chemistry, and meteorological conditions (Seinfeld and Pandis, 2016). Atmospheric $PM_{2.5}$ has known important environmental impacts related to visibility degradation and climate change. Because of their abilities to scatter and absorb solar radiation, aerosols degrade visibility in both remote and urban locations and can have direct and indirect effects on the climate (IPCC, 2013). Fine atmospheric particles are also a health concern and have been linked to respiratory and cardiovascular diseases (Sun et al., 2010; Viana et al., 2008; Zhang et al., 2014a). The magnitudes of the effects of $PM_{2.5}$ on all these systems depend on their sizes and chemical compositions. Highly reflective aerosols, such as sulfates and nitrates, result in direct cooling effects, while aerosols with low single-scattering albedos absorb solar radiation and include light-absorbing carbon, humic-like substances, and some components of mineral soils (Hoffer et al., 2006). The health impacts of these particles may also differ with different aerosol compositions (Zimmermann, 2015); the adverse health effects specifically associated with organic aerosols have been reported by Mauderly and Chow (2008). Therefore, the uncertainties surrounding the roles of aerosols in climate, visibility, and health studies can be significant because chemical composition data may not be available for large spatial and temporal ranges.

Reducing the uncertainties associated with aerosol effects requires observations of aerosol mass concentrations and chemical speciation from long-term spatially extensive ground-based networks. Continental sampling using ground-based networks has been conducted in North America (Hand et al., 2012) and Europe (Putaud et al., 2010) since the 1980s, such as via the U.S. EPA's Chemical Speciation Network (CSN), the Interagency Monitoring of Protected Visual Environments

(IMPROVE) network, the Clean Air Status and Trends Network (CASTNET) and the National Atmospheric Deposition Program (NADP). Previous studies suggest the spatial and temporal patterns of $PM_{2.5}$ mass concentrations and chemical species can vary significantly depending on species and location. For example, Malm et al. (2004) reported the 2001 monthly mean speciated aerosol concentrations from the IMPROVE monitors across the United States and demonstrated that ammonium sulfate concentrations were highest in the eastern United States and dominated the fine particle masses in the summer. Clearly decreasing gradients of the SO_4^{2-} and NO_3^- contributions to PM_{10} were observed in Europe when moving from rural to urban to kerbside sites (Putaud et al., 2010). Although large disparities of $PM_{2.5}$ pollution levels exist between those megacities in developing and developed countries, the $PM_{2.5}$ annual mass concentrations in the former are approximately 10 times greater than those of the latter (Cheng et al., 2016); however, ground-based networks that consistently measures $PM_{2.5}$ mass concentrations and chemical compositions remain rare in the densely populated regions of developing countries.

China is the world's most populous country and has one of the fastest-growing economies. Fast urbanization and industrialization can cause considerable increases in energy consumption. China's energy consumption increased 120% from 2000 to 2010. Coal accounted for most of the primary energy consumption (up to 70%) (Department of Energy Statistics, National Bureau of Statistics of China, 2001; 2011). Meanwhile, the emissions of high concentrations of numerous air pollutants cause severe air pollution and haze episodes. For example, a heavy air pollution episode occurred in northeastern China in January of 2013, wherein the maximum hourly averaged $PM_{2.5}$ exceeded 600 μgm^{-3} in Beijing (Wang et al., 2014). This event led to considerable public concern. However, ground-based networks that consistently measure $PM_{2.5}$ mass concentrations and chemical compositions in China are limited. Although there were some investigations of the various aerosol chemical compositions in China (He et al., 2001; Huang et al., 2013; Li et al., 2012; Liu et al., 2015; Pan et al., 2013; Tao et al., 2014; Wang et al., 2013; Yang et al., 2011; Zhao et al., 2013a; Zhou et al., 2012), earlier studies were limited in their temporal and spatial scopes, with very few having data exceeding one year while covering various urban and remote regions of the country (Zhang et al., 2012; Wang et al., 2015b). Indeed, before 2013, the Chinese national monitoring network did not report measurements of $PM_{2.5}$ or its chemical composition, and thus, ground-based networks for atmospheric fine particulate matter measurements at regional and continental scales are needed as these networks are essential for the development and implementation of effective air pollution control strategies and are also useful for the evaluation of regional and global models and satellite retrievals.

To meet these sampling needs, the "Campaign on atmospheric Aerosol REsearch" network of China (CARE-China) was established in late 2011 for the study of the spatiotemporal distributions of the physical and chemical characteristics and optical properties of aerosols (Xin et al., 2015). This study presents the first long-term dataset to include three years of observations of online $PM_{2.5}$ mass concentrations (2012-2014) and one year of observations of $PM_{2.5}$ compositions (2012-2013) from the CARE-China network. The purpose of this work is to (1) assess the $PM_{2.5}$ mass concentration levels, including the seasonal and diurnal variation characteristics at the urban, rural and regional background sites; to (2) obtain the seasonal variations of the $PM_{2.5}$ chemical compositions at paired urban/background sites in the most polluted regions and clean areas; and to

(3) identify the occurrences and chemical signatures of haze events via an analysis of the temporal evolutions and chemical compositions of $PM_{2.5}$ on polluted days. These observations and analyses provide general pictures of atmospheric fine particulate matter in China and can also be used to validate model results and implement effective air pollution control strategies.

2 Materials and methods

2.1 An introduction to the $PM_{2.5}$ monitoring sites

The $PM_{2.5}$ data from 36 ground observation sites used in this study were obtained from the CARE-China network (Campaign on the atmospheric Aerosol REsearch network of China), which was supported by the Chinese Academy of Sciences (CAS) Strategic Priority Research Program grants (Category A). Xin et al. (2015) provided an overview of the CARE-China network, the cost-effective sampling methods employed and the post-sampling instrumental methods of analysis. Four more ground observation sites (Shijiazhuang, Tianjin, Ji'nan and Lin'an) from the "Forming Mechanism and Control Strategies of Haze in China" group (Wang et al., 2014) were also included in this study to better depict the spatial distributions and temporal variations of the $PM_{2.5}$ in eastern China. A comprehensive 3-year observational network campaign from 2012 to 2014 was carried out at these 40 ground observation sites. Figure 1 and Table 1, respectively, show the geographic distribution and details of the network stations, which include 20 urban sites, 12 background sites and 8 rural/suburban sites. The urban sites, such as those at Beijing, Shanghai and Guangzhou, are locations surrounded by typical residential areas and commercial districts. The background sites are located in natural reserve areas or scenic spots, which are far away from anthropogenic emissions and are less influenced by human activities. Rural/suburban sites are situated in rural and suburban areas, which may be affected by agricultural activities, vehicle emissions and some light industrial activities. These sites are located in different parts of China and can provide an integrated insight into the characteristic of $PM_{2.5}$ over China.

2.2 Online instruments and data sets

A tapered element oscillating microbalance (TEOM) was used for the $PM_{2.5}$ measurements at thirty-four sites within the network (Table S1). This system was designated by the US Environmental Protection Agency (USEPA) as having a monitoring compliance equivalent to the National Ambient Air Quality standard for particulate matter (Patashnick and Rupprecht 1991). The measurement ranges of the TEOMs were 0-5 g/m^3, with a 0.1 μg/m^3 resolution and precisions of ±1.5 (1-h average) and ±0.5 μg/m^3. The models used in the network are TEOM 1400a and TEOM 1405, and the entire system was heated to 50 °C; thus, a loss of semi-volatile compounds cannot be avoided. Our previous study showed that up to 25% lower mass concentrations were found for select daily means than those observed with gravimetric filter measurements, depending on the ammonium-nitrate levels and ambient temperatures (Liu et al., 2015). The errors of the TEOM measurements are systematic in that they are always negative. Thus, these errors may not be important for the study of the spatial distributions and temporal variations of $PM_{2.5}$. The other six sites of the network (Shanghai, Guangzhou, Chengdu, Xi'an, Urumchi and Qinghai Lake) were equipped with beta gauge instruments (EBAM, Met One Instruments Inc., Oregon). The measurement range of EBAM is 0-1000 μg/m^3, with a precision of 0.1 μg/m^3 and a resolution of 0.1 μg/m^3. The filters were changed every week, and the inlet was cleaned every month. The flow rates were also monitored and concurrently calibrated. A year-long intercomparison of daily $PM_{2.5}$ mass

concentrations measured by TEOM and EBAM was conducted at the Beijing site (Fig. S1a), and the results showed that these two on-line instruments correlated well (R^2=0.90, P<0.01). TEOM reported approximately 24% lower mass concentration than EBAM, and the difference could be explained by the loss of semi-volatile materials from TEOM (Zhu et al., 2007).

2.3 Filter sampling and chemical analysis

In this study, filter sampling was conducted at the five urban sites of Beijing, Guangzhou, Lhasa, Shenyang and Chongqing as well as at the six background sites of Xinglong, Lin'an, Dinghu Mountain, Namsto, Changbai Mountain and Gongga Mountain. The Automatic Cartridge Collection Unit (ACCU) system of Rupprecht & Patashnick Co. with 47 mm diameter quartz fiber filters (Pall Life Sciences, Ann Arbor, MI, USA) was deployed in Beijing to collect the $PM_{2.5}$ samplers (Liu et al., 2016a). Similar to the ACCU system, a standard 47 mm filter holder with quartz fiber filters (Pall Life Sciences, Ann Arbor, MI, USA) was placed in the bypass line of TEOM 1400a and TEOM 1405 using quick-connect fittings and was used to collect the $PM_{2.5}$ samplers of the other nine sites, excepting Guangzhou and Lin'an. Each set of the $PM_{2.5}$ samples was continuously collected over 48 h on the same days of each week, generally starting at 8:00 a.m. The flow rates were typically 15.6 L/min. For the Guangzhou site, the fine particles were collected on Whatman quartz fiber filters using an Andersen model SA235 sampler (Andersen Instruments Inc.) with an air flow rate of 1.13 m^3/min. The sampling lasted 48h for the first three samples and 24 h for the rest samples, generally starting at 8:00 a.m. For the Lin'an site, a medium volume $PM_{2.5}$ sampler (Model: TH-150CIII, Tianhong Instrument CO., Ltd. Wuhan, China) was used to collect 24 h of $PM_{2.5}$ aerosols on 90 mm quartz fiber filters (QMA, Whatman, UK) once every 6 days (Xu et al., 2017). The sampling periods of these 11 urban and background sites are shown in Table S1.

All the filters were heat treated at 500 °C for at least 4 h for cleaning prior to filter sampling. The $PM_{2.5}$ mass concentrations were obtained via the gravimetric method with an electronic balance with a detection limit of 0.01 mg (Sartorius, Germany) after stabilizing at a constant temperature (20±1 °C) and humidity (45%±5%). $PM_{2.5}$ mass concentrations measured by gravimetric method correlated well with the on-line instruments (TEOM and EBAM) as showed in Fig. S1b. On average, $PM_{2.5}$ mass concentrations measured by the filter sampling was approximately 9% higher than the on-line instruments. Three types of chemical species were measured using the methods described in Xin et al. (2015). Briefly, the organic carbon (OC) and elemental carbon (EC) values were determined using a thermal/optical reflectance protocol using a DRI model 2001 carbon analyzer (Atmoslytic, Inc., Calabasas, CA, USA) with the thermal/optical reflectance (TOR) method. A circle piece of 0.495 cm^2 was cut off from the filters and was sent into the thermal optical carbon analyzer. In a pure helium atmosphere, OC1, OC2, OC3 and OC4 are produced stepwise at 140 ℃, 280 ℃, 480 ℃ and 580 ℃, respectively; followed by EC1 (540 ℃), EC2 (780 ℃) and EC3 (840 ℃) in a 2% oxygen-contained helium atmosphere. Eight main ions, including K^+, Ca^{2+}, Na^+, Mg^{2+}, NH_4^+, SO_4^{2-}, NO_3^- and Cl^-, were measured via ion chromatography (using a Dionex DX 120 connected to a DX AS50 autosampler for anions and a DX ICS90 connected to a DX AS40 autosampler for cations). One-quarter of each filter substrate was extracted with 25 mL deionized water in a PET vial for 30 min. Before performing a targeted sample analysis, a standard solution and blank test were performed, and the correlation coefficient of the standard samples was more than 0.999. The detection limits for all anions and cations, which were calculated as three times the standard

deviations of seven replicate blank samples, are all lower than 0.3 μg m^{-3} (Liu et al., 2017). The microwave acid digestion method was used to digest the filter samples into liquid solution for elemental analysis. One quarter of each filter sample was placed in the digestion vessel with a mixture of 6 mL HNO_3, 2 mL H_2O_2 and 0.6 mL HF, and was then exposed to a three-stage microwave digestion procedure from a microwave-accelerated reaction system (MARS, CEM Corporation, USA). After that, 18 elements, including Mg, Al, K, Ca, V, Cr, Mn, Fe, Co, Ni, Cu, Zn, As, Se, Ag, Cd, Tl and Pb, were determined by Agilent 7500a inductively coupled plasma mass spectrometry (ICP-MS, Agilent Technologies, Tokyo, Japan). Quantification was carried out by the external calibration technique using a set of external calibration standards (Agilent Corporation) at concentration levels close to that of the samples. The relative standard deviation for each measurement (repeated twice) was within 3%. The method detection limits (MDLs) were determined by adding 3 standard deviations of the blank readings to the average blank values (Yang et al., 2009). Quality control and quality assurance procedures were routinely applied for all the carbonaceous, ion and elemental analysis.

3. Results and discussions

3.1 Characteristics of $PM_{2.5}$ mass concentrations at urban and background sites

3.1.1 Average $PM_{2.5}$ levels

The location, station information and average $PM_{2.5}$ concentrations from the 40 monitoring stations are shown in Fig. 1 and Table 1. The highest $PM_{2.5}$ concentrations were observed at the urban stations of Xi'an (125.8 μg/m^3), Taiyuan (111.5 μg/m^3), Ji'nan (107.5 μg/m^3) and Shijiazhuang (105.1 μg/m^3), which are located in the most polluted areas of the Guanzhong Plain (GZP) and the North China Plain (NCP). Several studies have revealed that the enhanced $PM_{2.5}$ pollutions of the GZP and NCP are not only due to the primary emissions from local sources such as the local industrial, domestic and agricultural sources but are also due to secondary productions (Huang et al., 2014; Guo et al., 2014; Wang et al., 2014). Furthermore, the climates of the GZP and NCP are characterized by stagnant weather with weak winds and relatively low boundary layer heights, leading to favorable atmospheric conditions for the accumulation, formation and processing of aerosols (Chan and Yao, 2008). Note that the averaged $PM_{2.5}$ concentrations in Beijing and Tianjin were approximately 70 μg/m^3, which is much lower than those of the other cities, including Ji'nan and Shijiazhuang in the NCP, possibly because Beijing and Tianjin are located in the northern part of the NCP, far from the intense industrial emission area that is mainly located in the southern part of the NCP. Interestingly, the average $PM_{2.5}$ concentrations at Yucheng (102.8 μg/m^3) and Xianghe (83.7 μg/m^3) were even higher than most of those from the urban stations. Although Yucheng is a rural site, it is located in an area with rapid urbanization near Ji'nan and is therefore subjected to the associated large quantities of air pollutants. In addition, Xianghe is located between Beijing and Tianjin and is influenced by the regionally transported contributions from nearby megacities and the primary emissions from local sources. Yantai is a coastal city with relatively low PM concentrations compared to those of with inland cities on the NCP.

The $PM_{2.5}$ concentrations were also high in the Yangtze River Delta (YRD), which is another developed and highly-populated city cluster area like the NCP (Fu et al., 2013). The average $PM_{2.5}$ values of the three urban stations of Shanghai, Wuxi and Hefei were 56.2, 65.2 and 80.4 μg/m^3,

respectively, which are comparable to those of the megacities of Beijing and Tianjin in the NCP. Due to the presence of fewer coal-based industries and dispersive weather conditions, the $PM_{2.5}$ concentrations of the Pearl River Delta (PRD) are generally lower than those of the other two largest city clusters in China, such as those from the NCP and YRD. The average $PM_{2.5}$ value at Guangzhou was 44.1 μg/m^3, which was similar to the $PM_{2.5}$ values of the background stations from the NCP and YRD. Shenyang, the capital of the province of Liaoning, is located in the Northeast China Region (NECR), which is an established industrial area. High concentrations of trace gases and aerosol scattering in the free troposphere have been observed via aircraft observations and are due to regional transports and heavy local industrial emissions (Dickerson et al., 2007). In the present study, the average $PM_{2.5}$ concentration of Shenyang was 77.6 μg/m^3. Meanwhile, Hailun, which is a rural site in northeastern China, had an average $PM_{2.5}$ concentration of 41.6 μg/m^3, which was much lower than that of the rural site of Yucheng in the NCP.

High aerosol optical depths and low visibilities have been observed in the Sichuan Basin (Zhang et al., 2012), which is located in the Southwestern China Region (SWCR). The poor dispersion conditions and heavy local industrial emissions make this another highly polluted area in China. In the present study, the average $PM_{2.5}$ concentration in Chengdu was measured as 102.2 μg/m^3, which is much higher than the averages from the megacities of Beijing, Shanghai and Guangzhou but is comparable to those of Ji'nan and Shijiazhuang. Chongqing, another megacity located in the SWCR, however, showed much lower $PM_{2.5}$ values than Chengdu. Urumqi, the capital of the Uighur Autonomous Region of Xinjiang, located in northwestern China, experiences air pollution due to its increasing consumption of fossil fuel energy and steadily growing fleet of motor vehicles (Mamtimin and Meixner, 2011). The average $PM_{2.5}$ concentration measured in Urumqi is 104.1 μg/m^3, which is comparable to those of the urban sites in the GZP and NCP. The similarity among the $PM_{2.5}$ values for Cele, Dunhuang and Fukang is due to their location, being far from regions with intensive economic development but strongly affected by sandstorms and dust storms due to their proximity to dust source areas. For example, the average $PM_{2.5}$ concentration in Cele during the spring (200.7 μg/m^3) was much greater than those of the other three seasons. Lhasa, the capital of the Tibet Autonomous Region (TAR), is located in the center of the Tibetan Plateau at a very high altitude of 3700 m. The $PM_{2.5}$ concentrations in Lhasa were low, with average values of 30.6 μg/m^3, because of its relatively small population and few industrial emissions.

Much lower $PM_{2.5}$ concentrations were observed at the background stations, the values of which ranged from 11.2 to 46.5 μg/m^3. The lowest concentration of $PM_{2.5}$ was observed in Namsto, a background station on the TAR with nearly no anthropogenic effects. The highest $PM_{2.5}$ concentration of the background stations was observed at Lin'an, a background station in the PRD. The average $PM_{2.5}$ concentration at the urban and background sites in this study are shown as box-plots in Fig. S2a. The average $PM_{2.5}$ concentration of the background stations (a total of 12 sites) is 28.5 μg/m^3, and the average concentration of the $PM_{2.5}$ values from urban stations (a total of 20 sites) is 73.2μg/m^3. The latter value is approximately three times the former, suggesting the large differences in fine particle pollution at urban and background sites across China. To further characterize these kinds of differences for different parts of China, six pairs of $PM_{2.5}$ values measured from urban and background stations were selected to represent the NCP, YRD, PRD, TAR, NECR and SWCR, respectively (Fig. S2). The first three areas (NCP, YRD and PRD) and the last

two areas (NECR and SWCR) were the most industrialized and populated regions in China, while TAR is the cleanest area in China. The $PM_{2.5}$ concentrations of the background stations in the NCP, YRD and PRD are 39.8 μg/m^3 (Xinglong), 46.5 μg/m^3 (Lin'an) and 40.1 μg/m^3 (Dinghu Mountain) and are much higher than those of the background stations in other parts of China, which are usually below 25 μg/m^3. All values especially for those observed in urban and rural sites in this study were much greater than the results from Europe and North America. For urban/suburban sites, average $PM_{2.5}$ concentrations of 20.1 μg/m^3 was reported by Gehrig and Buchmann (2003) from 1998 to 2001 in Switzerland, and average concentrations of 16.3 μg/m^3 for the period 2008-2009 in the Netherlands (Janssen et al., 2013). Between October 2008 and April 2011, the 20 study areas covered major cities of the European ESCAPE project showed annual average concentrations of $PM_{2.5}$ ranging from 8.5 to 29.3 μg/m^3, with low concentrations in northern Europe and high concentrations in southern and eastern Europe (Eeftens et al., 2012). Based on a constructed database of $PM_{2.5}$ component concentrations from 187 counties in the United States for 2000-2005, Bell et al. (2007) reported an average $PM_{2.5}$ value of 14.0 μg/m^3, with higher values in the eastern United States and California, and lowest values in the central regions and Northwest. For background sites, Putaud et al. (2010) showed that annual average of $PM_{2.5}$ ranged from 3 to 22μg/m^3 observed from 12 background sites across Europe. In addition, average $PM_{2.5}$ value of 12.6μg/m^3 was observed at a regional background site in the Western Mediterranean from 2002 to 2010 (Cusack et al., 2012).

3.1.2 Seasonal variations of $PM_{2.5}$ mass concentrations

Generally, the $PM_{2.5}$ concentrations in urban areas show distinct seasonal variabilities, with maxima during the winter and minima during the summer for most of China (Fig. 1), which is a similar pattern to that of the results reported by Zhang and Cao (2015). In northern and northeastern China, the wintertime peak values of $PM_{2.5}$ were mainly attributed to the combustion of fossil fuels and biomass burning for domestic heating over extensive areas, which emit large quantities of primary particulates as well as the precursors of secondary particles (He et al., 2001). In addition, new particle formation and the secondary production of both inorganic aerosols and OM could further enhance fine PM abundance (Huang et al., 2014; Guo et al., 2014). Furthermore, the planetary boundary layer is relatively low in the winter, and more frequent occurrences of stagnant weather and intensive temperature inversions cause very bad diffusion conditions, which can result in the accumulation of atmospheric particulates and lead to high-concentration PM episodes (Quan et al., 2014; Zhao et al., 2013b). In southern and eastern China, although the effect of domestic heating is not as important as that in northern China, the weakened diffusion and transport of pollutants from the north due to the activity of the East Asian Winter Monsoon reinforces the pollution from large local emissions in the winter more than in any other season (Li et al., 2011; Mao et al., 2017). For northwestern and West Central China, the most polluted season is the spring instead of the winter due to the increased contribution from dust particles in this desert-like region (Zou and Zhai, 2004), suggesting that the current $PM_{2.5}$ control strategies (i.e., reducing fossil/non-fossil combustion derived VOCs and PM emissions) will only partly reduce the $PM_{2.5}$ pollution in western of China. $PM_{2.5}$ is greatly decreased during the summer in urban areas, which is associated with the reduced anthropogenic emissions from fossil fuel combustion and biomass burning domestic heating. Further, the more intense solar radiation causes a higher atmospheric mixing layer,

which leads to strong vertical and horizontal aerosol dilution effects (Xia et al., 2006). In addition, increased precipitation in most of China due to the summer monsoon can increase the wet scavenging of atmospheric particles. As a result, $PM_{2.5}$ minima are observed in the summer at urban sites.

The seasonal variations of $PM_{2.5}$ at the background sites varied in different parts of China (Fig. 3). Dinghu Mountain and Lin'an showed maximum values in the winter, while Zangdongnan, Qinghai Lake, Xishuangbanna and Mount Everest showed maximum values in the spring. In addition, a summer maximum of $PM_{2.5}$ was observed for Xinglong, and an autumn maximum was observed for Tongyu. Changbai Mountain, Gongga Mountain and Namsto showed weak seasonal variabilities. These results suggest the different contributions from regional anthropogenic and natural emissions and long-range transports to background stations. The monthly average $PM_{2.5}$ concentrations of the urban and background sites in the NCP, YRD, PRD, TAR, NECR and SWCR are further analyzed and shown in Fig. 2. The monthly variations of the $PM_{2.5}$ concentrations at the background sites in the YRD and PRD were consistent with those of the nearby urban sites, both of which showed maximum values in December (YRD) and January (PRD). The reasons for this similarity are primarily the seasonal fluctuations of emissions, which are already well known due to the similar variations of other parameters, including sulfur dioxide and nitrogen oxide, as shown in Fig. S3. In contrast, the monthly variations of $PM_{2.5}$ at Xinglong showed different trends than those of the nearby urban stations. The maximum value of $PM_{2.5}$ at this site was observed in July, while the maximum value in Beijing was observed in January. The reasons for this are not primarily the seasonal fluctuations of emissions, but rather meteorological effects (frequent inversions during the winter and strong vertical mixing during the summer). The Xinglong site is situated at an altitude of 900 m a.s.l., and therefore, during the wintertime, the majority of cases above the inversion layer are protected from the emissions of the urban agglomerations of the NCP. Furthermore, in the NCP area, northerly winds prevail in the winter, while southerly winds prevail in the summer. Thus, in the summer, more air masses from the southern urban agglomerations will lead to high $PM_{2.5}$ concentrations in Xinglong. Weak monthly variabilities were observed for Namsto, Changbai Mountain and Gongga Mountain, although remarkable monthly variabilities were found at the nearby cities of Lhasa, Shenyang and Chongqing. The reasons for this difference are mainly that these three sites are elevated remote stations that are far from human activities and show predominant meteorological influences.

3.1.3 Diurnal variations of $PM_{2.5}$ mass concentrations

To derive importance information to identify the potential emission sources and the times when the pollution levels exceed the proposed standards, hourly data were used to examine the diurnal variabilities of $PM_{2.5}$ as well as those of the other major air pollutants. Fig. 3 illustrates the diurnal variations of the hourly $PM_{2.5}$ concentrations in Beijing, Shanghai, Guangzhou, Lhasa, Shenyang and Chongqing, in the largest megacities in the NCP, YRD, PRD, TAR, NECR and SWCR and in the different climatic zones of China, respectively. Of the urban sites, Lhasa has the lowest $PM_{2.5}$ concentrations, but the most significant pronounced diurnal variations of $PM_{2.5}$, with obvious morning and evening peaks appearing at 10:00 and 22:00 (Beijing Time) due to the contributions of enhanced anthropogenic activity during the rush hours. The minimum value occurred at 16:00, which is mainly due to a higher atmospheric mixing layer, which is beneficial for air pollution

diffusion. This bimodal pattern was also observed in Shenyang and Chongqing, which show morning peaks at 7:00 and 9:00 and evening peaks at 19:00 and 20:00, respectively. However, the $PM_{2.5}$ values in Beijing, Shanghai and Guangzhou showed much weaker urban diurnal variation patterns, and slightly higher $PM_{2.5}$ concentrations during the night than during the day were observed, which can be explained by the enhanced emissions from heating and the relatively low boundary layer. Moreover, fine particles emitted from diesel truck traffic which is allowed only during nighttime would additionally increase $PM_{2.5}$ burden because emission factors of heavy-duty vehicles are 6 times than those from light-duty vehicles (Westerdahl et al., 2009). Note that the morning peaks in Beijing, Shanghai and Guangzhou were not as obvious as those of other cities, although both the SO_2 and NO_2 values increased due to increased anthropogenic emissions (Fig. S4). Alternatively, this decreasing trend may be the result of an increasing boundary layer depth. The invisible morning peak of $PM_{2.5}$ in these three cities was possibly attributed to the stricter emission standards applied at recently years. As showed in Fig.S5, the morning peak of $PM_{2.5}$ in Beijing was gradually disappeared or invisible after National 5 vehicle emission standard applied at the beginning of 2013 (www.bjpc.gov.cn). The same thing would be also observed in Shanghai and Guangzhou which implemented the same vehicle emission standards followed Beijing, while it not true for the other cities as the latest vehicle emission standard was usually applied 2-3 years later than the three megacities. At the urban sites of Beijing, Shanghai and Guangzhou, the $PM_{2.5}$ levels started to increase in the late afternoon, which could be explained by the increasing motor vehicle emissions as NO_2 is also dramatically increased during the same period.

At the background area of the TAR, significant pronounced diurnal variations of $PM_{2.5}$ were observed in Namsto, with a morning peak at 9:00 and an evening peak at 21:00 (Fig. 3d), which are similar to those of the urban site of Lhasa. As there are hardly any anthropogenic activities near Namsto, this kind of diurnal pattern of $PM_{2.5}$ may be influenced by the evolution of the planetary boundary layer. Both Gongga Mountain and Lin'an showed the same bimodal pattern of $PM_{2.5}$ as that in Namsto, the former site could also be influenced by the planetary boundary layer, while the latter site was not only influenced by the evolution of the planetary boundary layer but also would be highly affected by the regional transportation from the YRD region. For the background site of the NCP, however, Xinglong showed smooth $PM_{2.5}$ variations. As mentioned before, the Xinglong station is located on the mountain and has an altitude of 960 m a.s.l. The mixed boundary layer of the urban area increases in height in the morning and reaches a height of approximately 1000 meters in the early afternoon. Then, the air pollutants from the urban area start to affect the station as the vertical diffusion of the airflow and the $PM_{2.5}$ concentration reach their maxima at 18:00. Next, the concentration starts to decrease when the mixed boundary layer collapses in the late afternoon, eventually forming the nocturnal boundary layer (Boyouk et al., 2010). Thus, $PM_{2.5}$ concentration decreased slowly during the night and morning, reaching a minimum at 10:00. At Dinghu Mountain and Changbai Mountain, the daytime $PM_{2.5}$ greater than that of the nighttime, with a maximum value occurring at approximately 11:00-12:00. This kind of diurnal pattern of $PM_{2.5}$ is mainly determined by the effects of the mountain-valley breeze. Both the Dinghu Mountain and Changbai Mountain stations are located near the mountain. Thus, during daytime, the valley breeze from urban areas carries air pollutants that will accumulate in front of the mountain and cause an increase of the PM concentration. Meanwhile, at night, the fresh air carried by the mountain breeze will lead to the

dilution of the PM, so low concentrations are sustained during the night. Further support for this pattern comes from the much higher maximum values of $PM_{2.5}$ in the winter than those in the summer, as enhanced air pollutant emissions in urban areas are expected in the winter due to heating.

3.2 Chemical compositions of $PM_{2.5}$ in urban and background sites

3.2.1 Overview of $PM_{2.5}$ mass speciation

Figure 4 shows the annual average and seasonal average chemical compositions of $PM_{2.5}$ at six urban and six background sites, which represent the largest megacities and regional background areas of the NCP, YRD, PRD, TAR, NECR and SWCR. The chemical species of $PM_{2.5}$ in Shanghai were obtained from Zhao et al. (2015). The atmospheric concentrations of the main $PM_{2.5}$ constituents are also shown in Table 2. The EC, nitrate (NO_3^-), sulfate (SO_4^{2-}), ammonium (NH_4^+) and chlorine (Cl^-) concentrations were derived directly from measurements. Organic matter (OM) was calculated assuming an average molecular weight per carbon weight, showing an OC of 1.6 at the urban sites and of 2.1 at the background sites, based on the work of Turpin and Lim (2001); however, these values are also spatially and temporally variable, and typical values could range from 1.3 to 2.16 (Xing, et al., 2013). The calculation of mineral dust was performed on the basis of crustal element oxides (Al_2O_3, SiO_2, CaO, Fe_2O_3, MnO_2 and K_2O). In addition, the Si content, which was not measured in this study, was calculated based on its ratio to Al in crustal materials (Mason, 1966); namely, [Si]=3.41×[Al]. Finally, the unaccounted-for mass refers to the difference between the $PM_{2.5}$ gravimetric mass and the sum of the PM constituents mentioned above.

The PM constituents' relative contributions to the PM mass are independent of their dilutions and reflect differences in the sources and processes controlling the aerosol compositions (Putaud et al., 2010). When all the main aerosol components except water are quantified, they account for 73.6-84.8% of the $PM_{2.5}$ mass (average 79.2%) at urban sites and for 76.2-91.1% of the $PM_{2.5}$ mass (average 83.4%) at background sites. The remaining unaccounted-for mass fraction may be the result of analytical errors, a systematic underestimation of the PM constituents whose concentrations are calculated from the measured data (e.g., OM, and mineral dust), and aerosol-bound water (especially when mass concentrations are determined at RH >30%). For the urban sites, the mean composition given in descending concentrations is 26.0% OM, 17.7% SO_4^{2-}, 11.8% mineral dust, 9.8% NO_3^-, 6.6% NH_4^+, 6.0% EC and 1.2% Cl^-. For the background sites, the mean composition given in descending concentrations is 33.2% OM, 17.8% SO_4^{2-}, 10.1% mineral dust, 8.7% NH_4^+, 8.6% NO_3^-, 4.1% EC and 0.9% Cl^-. Generally, the chemical compositions of the $PM_{2.5}$ at background sites are similar to those of the urban sites, although they show a much higher fraction of OM and lower fractions of NO_3^- and EC. Significant seasonal variations of the chemical compositions were observed at urban sites (Fig. 4c), with much higher fractions of OM (33.7%) and NO_3^- (11.1%) in the winter and much lower fractions of OM (20.7%) and NO_3^- (6.9%) in the summer. In contrast, the fraction of SO_4^{2-} was consistent among the different seasons, although its absolute concentration in the winter (14.9 μg/m^3) was higher than that in the summer (11.7 μg/m^3). Compared with those at urban sites, different seasonal variation of OM were observed at the background sites, which showed summer maxima and winter/spring minima (Fig. 4d). While the wintertime peaks of OM at the urban sites were probably due to additional local emissions sources related to processes like heating, the summer peaks at the background sites were attributed to the enhanced biogenic emissions. Note that the seasonal variations of NO_3^- were similar to those at urban sites; this seasonal

phenomenon is due to the favorable conditions of cold temperature and high relative humidity conditions leading to the formation of particulate nitrate. The seasonal behaviors of SO_4^{2-} at the background sites were markedly different than those of the urban sites and indicate very different sources and atmospheric processing of SO_4^{2-}, which will be further discussed for specific regions of China.

There are significant variations of the absolute speciation concentrations at these urban and background sites (Table 2). For the urban sites, the OM concentrations span a 2-fold concentration range from 12.6 μg/m^3 (Lhasa) to 23.3 μg/m^3 (Shenyang), while these values range from 3.4 μg/m^3 (Namtso) to 21.7 μg/m^3 (Lin'an) at the background sites. The SO_4^{2-} and NO_3^- concentrations exhibit larger spatial heterogeneities than those of the OM for both urban and background sites. The absolute values of SO_4^{2-} have an approximately 25-fold range in urban sites, from 0.8 μg/m^3 (Lhasa) to 19.7 μg/m^3 (Chongqing), while this value has a 30-fold range at the background sites, from 0.4 μg/m^3 (Namsto) to 11.2 μg/m^3 (Lin'an). The corresponding mass fractions are 26.8% in Chongqing and below 3% in Lhasa. Much higher fractions of SO_4^{2-} in the $PM_{2.5}$ were observed at the urban sites located in southern China than those in northern China, although the average concentration of $PM_{2.5}$ is greater in the north than in the south, suggesting that sulfur pollution remains a problem for southern China (Liu, et al., 2016b). This problem may be attributed to higher sulfur contents of the coal in southern China, with 0.51% in the north vs. 1.32% in the south and up to >3.5% in Chongqing in southern China (Lu et al., 2010; Zhang et al., 2010). In addition, the higher fraction of sulfate in south China is also likely associated to the higher oxidation capacity in south China and therefore higher formation efficiency from SO_2 to SO_4^{2-}. The absolute values of NO_3^- have an approximately 20-fold range in urban sites and a greater than 100-fold range in background sites. This heterogeneity reflects the large spatial and temporal variations of the NO*x* sources. For the urban sites, the absolute EC values have a 5-fold concentration range, from 1.4 μg/m^3 (Lhasa) to greater than 7.0 μg/m^3 (Guangzhou), while this species has a 15-fold concentration range at the background sites and is mainly from anthropogenic sources. In comparison, the absolute concentrations of mineral dust exhibit much weaker spatial variations at the urban and background sites.

The characteristics of the $PM_{2.5}$ chemical compositions at individual site were discussed in more detail. In this section, six pairs of urban and background sites from each region of China were selected, and the differences in the chemical compositions of urban and background sites were analyzed.

3.2.2 North China Plain

Beijing is the capital of China and has attracted considerable attention due to its air pollution (Chen et al., 2013). Beijing is the largest megacity in the NCP, which is surrounded by the Yanshan Mountains to the west, north and northeast and is connected to the Great North China Plain to the south. The filter sampler is located in the courtyard of the Institute of Atmospheric Physics (IAP) (116.37°E, 39.97°N), 8 km northwest of the center of downtown. The $PM_{2.5}$ concentration during the filter sampling period was 71.7 μg/m^3, which is close to the three-year average $PM_{2.5}$ value reported by TEOM (Table 1). $PM_{2.5}$ in Beijing is mainly composed by OM (26.6%), SO_4^{2-} (16.5%) and NO_3^- (13.0%) (Fig. 5a), which compare well with previous studies (Yang et al., 2011; Oanh et al., 2006). However, the mineral dust fraction found in this study (6.5%) was much lower than that found in Yang et al. (2011) (19%) but was comparable to that found in Oanh et al. (2006) (5%),

potentially due to difference in definitions. In addition, the EC fraction (5.7%) was slightly lower than those found in previous studies (7%-7.4%) (Yang et al., 2011; Wang et al., 2015a). The annual concentration of OM (19.1 μg/m^3) in Beijing was comparable to those in Shanghai, Guangzhou and Chongqing, but was much lower than that in Shenyang. Higher fractions of OM were observed in the winter (34.2%) and autumn (30.5%) than in the summer (21.6%) and spring (20.9%). The annual concentration of SO_4^{2-} (11.9 μg/m^3) was much lower than those of earlier years (15.8 μg/m^3, 2005-2006) (Yang et al., 2011), suggesting that the energy structure adjustment implemented in Beijing (e.g., replacing coal fuel with natural gas) has been effective in decreasing the particulate sulfate in Beijing. Further support for this comes from the SO_4^{2-} concentration in the winter (16.5 μg/m^3) being comparable to that in the summer (13.4 μg/m^3). The significant NO_3^- value (9.3 μg/m^3) reflects the significant urban NOx emissions in Beijing, which was greatest during the winter, as expected from ammonium-nitrate thermodynamics. The greater mineral component in the spring reflects the regional natural dust sources.

The filter sampling site in Xinglong (117.58°E, 40.39°N) was located at Xinglong Observatory, National Astronomical Observatory, Chinese Academy of Sciences, which is 110 km northeast of Beijing (Fig. 1). This site is surrounded by mountains and is minimally affected by anthropogenic activities. The $PM_{2.5}$ concentration during the filter sampling period was 42.6 μg/m^3, which is close to the three-year average $PM_{2.5}$ values reported by TEOM (Table 1). The annual chemical composition of the $PM_{2.5}$ in Xinglong was similar to that in Beijing, although relatively higher fractions of OM and sulfate were observed in Xinglong (Fig. 5a). Higher fractions of OM were found in the winter (36.7%), and higher fractions of sulfate were found in the summer (32.1%) than in any other season (OM: 23.0-30.4%; SO_4^{2-}: 15.7-20.1%). Interestingly, the summer SO_4^{2-} concentration in Xinglong (14.4 μg/m^3) was even higher than that in Beijing, suggesting spatially uniform distributions of SO_4^{2-} concentrations across the NCP. This result indicates that regional transport can be an important source of SO_4^2 aerosols in Beijing, especially during the summer.

3.2.3 Yangtze River Delta

Shanghai is the economic center of China, lying on the edge of the broad flat alluvial plain of the YRD, with a few mountains to the southwest. The filter sampler was located at the top of a four-floor building of the East China University of Science and Technology (121.52°E, 31.15°N) (Zhao et al., 2015), approximately 10 km northwest of the center of downtown. The $PM_{2.5}$ concentration during the filter sampling period was 68.4 μg/m^3, which is greater than the three-year average $PM_{2.5}$ value reported by EBAM, likely due to the different sampling period (Table S1). The $PM_{2.5}$ in Shanghai mainly comprises OM (24.9%), SO_4^{2-} (19.9%) and NO_3^- (17.4%), which is comparable to the results of previous studies (Ye et al., 2003; Wang et al., 2016). This site had the highest NO_3^- (11.9 μg/m^3) and the second-highest SO_4^{2-} (13.6 μg/m^3) values of the urban sites, while its OM (17.1 μg/m^3) was comparable to those of Guangzhou and Chongqing. The SO_4^{2-} and NO_3^- values were highest during the autumn as expected based on the widespread biomass burning in the autumn in the YRD (Niu et al., 2013). However, the OM values were highest during the winter and mainly originated from secondary aerosol processes based on the highest OC/EC ratios (6.0) and the poor relationship of the OC and EC in this season.

Filter sampling was conducted at the Lin'an Regional Atmospheric Background Station (119.73°E, 30.30°N), which is a background monitoring station for the World Meteorological

Organization (WMO) global atmospheric observation network. The Lin'an site was located at the outskirts of Lin'an County within Hangzhou Municipality, which was 200 km southwest of Shanghai (Fig. 1). This site is surrounded by agricultural fields and woods and is less affected by urban, industrial and vehicular emissions (Xu et al., 2017). The $PM_{2.5}$ concentration during the filter sampling period was 66.3 μg/m^3, which is higher than the three-year average $PM_{2.5}$ values reported by TEOM, likely due to the different sampling period (Table S1). The annual chemical composition of the $PM_{2.5}$ in Lin'an was different than that in Shanghai, with much higher fractions of OM (32.7%) and NH_4^+ (11.0%). Furthermore, the absolute concentration of OM in Lin'an was much higher than that in Shanghai, especially in the summer (21.7 vs. 9.9 μg/m^3), which may be attributed to the enhanced biomass burning at both local and regional scales as well as the higher concentration of summer EC in Lin'an than in Shanghai (2.2 vs. 1.4 μg/m^3). In addition, the SO_4^{2-} and NO_3^- concentrations in Lin'an were comparable to those in Shanghai. These results suggest a spatially homogeneous distribution of secondary aerosols over the PRD and the the transportation of aged aerosol and gas pollutants from city clusters has significantly changed the aerosol chemistry in the background area of this region.

3.2.4 Pearl River Delta

Guangzhou is the biggest megacity in south China located in the PRD and mainly consists of floodplains within the transitional zone of the East Asian monsoon system (Yang et al., 2011). The filter sampler was set up on the rooftop of a 15-m high building of the Guangzhou Institute of Geochemistry, Chinese Academy of Sciences (113.35°E, 23.12°N). This site was surrounded by heavily trafficked roads and dense residential areas, representing a typical urban location. The $PM_{2.5}$ concentration during the filter sampling period was 75.3 μg/m^3, which is much higher than the three-year average $PM_{2.5}$ value reported by EBAM (Table 1), likely due to the different sampling period and location. The $PM_{2.5}$ in Guangzhou mainly comprises OM (22.2%), SO_4^{2-} (17.3%) and mineral dust (9.7%), which have values comparable to previous studies conducted in the years of 2013-2014 (Chen et al., 2016; Tao et al., 2017). This site has the lowest OC/EC ratio (1.5) of all urban sites, which can be explained by the abundance of diesel engine truck in Guangzhou City (Verma et al., 2010). Obvious seasonal variations of OM, SO_4^{2-} and NO_3^- were observed, showing winter/autumn maxima and summer/spring minima. In addition, summer minima were also observed for EC and NH_4^+. High mixing heights in the summer and clean air masses affected by summer monsoons from the South China Sea should lead to the minima of these species in summer, while the low wind speeds, weak solar radiation, relatively low precipitation (Tao et al., 2014) and relatively high emissions (Zheng et al., 2009) result in the much higher concentrations of OM and secondary inorganic aerosols (SO_4^{2-}, NO_3^- and NH_4^+) in the winter and autumn.

Filter sampling was conducted at Dinghu Mountain Station (112.50°E, 23.15°N), which is located in the middle of Guangdong Province in southern China. This site was surrounded by hills and valleys, being approximately 70 km west of Guangzhou (Fig. 1). The $PM_{2.5}$ concentration during the filter sampling period was 40.1 μg/m^3, close to the three-year average $PM_{2.5}$ values reported by TEOM. Distinct seasonal variations of OM, SO_4^{2-}, NO_3^- and NH_4^+ were observed, with the highest concentration of OM and NO_3^- occurring in the winter, while the highest concentrations of $SO_4^{2-}$and NH_4^+ occurred in the autumn. In contrast, EC and mineral dust showed weak seasonal variations. Dinghu Mountain has the second-highest EC and SO_4^{2-} values of the background sites,

being 2.0 μg/m^3 and 10.1 μg/m^3. In addition, the lowest OC/EC ratio was observed at Dinghu Mountain (2.8); the other background sites had values ranging from 3.5-8.3. These results indicate that this background site is intensely influenced by vehicular traffic, fossil fuel combustion and industrial emissions due to the advanced urban agglomeration in the PRD region. These results are consistent with the finds from previous studies (Liu et al., 2011; Wu et al., 2016). Compared with those from Guangzhou, higher fractions of SO_4^{2-} and NO_3^- were observed at Dinghu Mountain, while the fractions of OM and mineral dust were similar at these two sites, possibly indicating that there was a significantly larger fraction of transported secondary aerosols or aged aerosols at the background site of the PRD.

3.2.5 Tibetan Autonomous Region

Located in the inland TAR, Lhasa is one of the highest cities in the world (at an altitude of 3700 m). The city of Lhasa is located in a narrow west-east oriented valley in the southern part of the TAR. The filter sampler was located on the roof of a 20-m high building on the campus of the Institute of Tibetan Plateau Research (Lhasa branch) (91.63°E, 29.63°N). This site is close to Jinzhu road, one of the busiest roads in the city (Cong et al., 2011). The $PM_{2.5}$ concentration during the filter sampling period was 36.4 μg/m^3, which is close to the three-year average $PM_{2.5}$ values reported by TEOM. The $PM_{2.5}$ in Lhasa mainly comprises OM (34.5%) and mineral dust (31.9%), and the secondary inorganic aerosols (SO_4^{2-}, NO_3^- and NH_4^+) contributed little to the $PM_{2.5}$ (<5%). These results are comparable to those of a previous study conducted in the year of 2013-2014 (Wan et al., 2016). In addition, this site reports the lowest OM (12.6 μg/m^3), secondary inorganic aerosols (1.7 μg/m^3) and EC (1.4 μg/m^3) values of the urban sites in this study. Higher fractions of OM were observed in the winter (48.4%) and spring (43.1%), exceeding those in the summer (24.6%) and autumn (31.2%). Weak seasonal variations were found for the SO_4^{2-} (1.5-3.0%) and NO_3^- (1.1-1.7%) values, suggesting the negligible contributions from fossil fuel combustion in Lhasa.

Filter sampling was conducted at the Namtso Monitoring and Research Station for Multisphere Interactions (90.98°E, 30.77°N), a remote site located on the northern slope of the Nyainqen-tanglha Mountains, approximately 125 km northwest of Lhasa (Fig. 1). The $PM_{2.5}$ concentration during the filter sampling period was 9.5 μg/m^3, which is close to the three-year average $PM_{2.5}$ value reported by TEOM. The $PM_{2.5}$ in Namtso mainly comprises mineral dust (40.8%) and OM (36.3%), while SO_4^{2-} and NO_3^- contributed less than 5% to the $PM_{2.5}$. This chemical composition is distinctly different from those of the other background sites in this study, but is comparable to the background site at Qinghai Lake in the TAR (Zhang et al., 2014b). Namtso has the lowest OM, EC, SO_4^{2-}, NO_3^- and NH_4^+ values of all the background sites in this study. Spring maxima and winter minima were observed for the OM and EC, while the SO_4^{2-}, NO_3^- and NH_4^+ values showed weak seasonal variations. The highest OC/EC ratio was observed (8.3) at this site, suggesting that the organic aerosols at Namtso mainly originated from secondary aerosol processes or aged organic aerosols from regional transports.

3.2.6 Northeast China Region

Shenyang is the capital city of Liaoning province and the largest city in northeastern China. The main urban area is located on a delta to the north of the Hun River. The filter sampler was located at the Shenyang Ecological Experimental Station of the Chinese Academy of Science (123.40°E, 41.50°N) and was surrounded by residential areas with no obvious industrial pollution

sources around the monitoring station, representing the urban area of Shenyang. The $PM_{2.5}$ concentration during the filter sampling period was 81.8 μg/m^3, which is close to the three-year average $PM_{2.5}$ value reported by TEOM (Table 1). The $PM_{2.5}$ in Shenyang mainly comprises OM (28.5%), SO_4^{2-} (16.1%) and mineral dust (11.3%). This site reports the highest OM (23.3 μg/m^3) and mineral dust (9.2 μg/m^3) values as well as the second-highest EC (5.2 μg/m^3) value of the urban sites. The NO_3^- concentration at this site, however, was the second-lowest of the urban sites (Table 2). Much higher fractions of OM were observed in the winter (40.5%) than in the other seasons (15.6-26.5%) (Fig. 5), possibly due to the enhanced coal burning for winter heating. Further support for this pattern comes from the high abundance of chlorine during the cold seasons, which is mainly associated with coal combustion. The contribution from sea-salt particles is not important since the sampling sites are at least 200 km from the sea. Note that the fraction of SO_4^{2-} in the $PM_{2.5}$ during the winter was lower than that in the summer, although the absolute concentration was much higher in the winter (23.6 μg/m^3) than in the summer (11.3 μg/m^3). This result may be attributed to the reduced transformation of sulfur dioxide at low temperatures.

Filter sampling was conducted at the Changbai Mountain forest ecosystem station (128.01°E, 42.40°N), which was mostly surrounded by hills and forest and is located approximately 390 km northeast of Shenyang (Fig. 1). This site is situated 10 km from the nearest town, Erdaobaihe, which has approximately 45000 residents. The sources of PM were expected to be non-local. Hence, this site is considered a background site in the NECR. The $PM_{2.5}$ concentration during the filter sampling period was 23.3 μg/m^3, which is close to the three-year average $PM_{2.5}$ value reported by TEOM (Table 1). The main contributions to the $PM_{2.5}$ at Changbai Mountain were OM (38.1%), mineral dust (16.0%) and SO_4^{2-} (14.3%), similar to those in Shenyang. Note that the summer OM concentrations were quite similar at these two sites (8.0 vs. 9.0 μg/m^3), but the OC/EC ratios were different (4.8 vs. 1.6), which may reflect the different origins of the OM at the urban (primary emissions) and background sites (secondary processes) of the NECR. The OM concentrations in the other seasons were much lower at Changbai Mountain than those from Shenyang city, especially during the winter (10.8 vs. 59.4 μg/m^3). In fact, weak seasonal variations of chemical species (OM, EC, SO_4^{2-}, NO_3^- and NH_4^+) were observed at Changbai Mountain. This site reports the second-lowest values of OM, EC, SO_4^{2-} and Cl^- of the background sites. These results suggest that aerosols at Changbai Mountain were influenced by the regional transports alone.

3.2.7 Southwestern China Region

Chongqing is the fourth municipality near Central China, lying on the Yangtze River in mountainous southwestern China, near the eastern border of the Sichuan Basin and the western border of Central China. For topographic reasons, Chongqing has some of the lowest wind speeds in China (annual averages of 0.9-1.6 m s^{-1} from 1979 to 2007; Chongqing Municipal Bureau of Statistics, 2008), which favors the accumulation of pollutants. The filter sampler was located on the rooftop of a 15-m high building on the campus of the Southwest University (106.54°E, 29.59°N). This site is located in an urban district of Chongqing with no obvious industrial pollution sources around the monitoring site, representing the urban area of Chongqing. The $PM_{2.5}$ concentration during the filter sampling period was 73.5 μg/m^3, of which 26.8% is SO_4^{2-}, 23.5% OM, 10.0% mineral dust, 8.9% NO_3^-, 8.2% EC and 6.5% NH_4^+. The OM fraction is smaller than those measured by Yang et al. (2011) (32.7%) and Chen et al., 2017 (30.8%), while the SO_4^{2-} fraction is greater than

the values reported in these two studies (19.8-23.0%). This site shows the highest SO_4^{2-} (19.7 μg/m^3), the highest NH_4^+ (6.1 μg/m^3) and the third-highest EC (4.8 μg/m^3) values of the urban sites. A weak seasonal variation in the chemical composition of $PM_{2.5}$ was observed, although a much higher concentration of this species was found in the winter than in the other seasons.

Filter sampling was performed at the Gongga Mountain Forest Ecosystem Research Station (101.98°E, 29.51°N) in the Hailuogou Scenic Area, a remote site located in southeastern Ganzi in the Tibetan Autonomous Prefecture in Sichuan province. This site is mostly surrounded by glaciers and forests and is located approximately 450 km northwest of Chongqing (Fig. 1). The $PM_{2.5}$ concentration during the filter sampling period was 32.2 μg/m^3, close to the three-year average $PM_{2.5}$ value reported by TEOM (Table 1). The dominant components of $PM_{2.5}$ were OM (40.7%), SO_4^{2-} (14.6%) and mineral dust (9.8%), similar to those at Changbai Mountain. This site has the second-highest OM (13.1 μg/m^3) value of the background sites, which may mainly be due to secondary processes, considering the high OC/EC ratio (5.6). In addition, distinct seasonal variations of OM were observed, which shows summer maxima (19.9 μg/m^3) and autumn minima (9.1 μg/m^3). Previous studies showed higher mixing ratios of the VOCs during the spring and summer and lower mixing ratios during the autumn at Gongga Mountain (Zhang et al., 2014c), which may result in high concentrations of OM in the summer because the OC/EC ratio reaches its highest value in the summer (10.3). Second-lowest EC and NO_3^- values of the background sites were observed here, suggesting the insignificant influence of human activities in this region.

3.3 Temporal evolution and chemical composition $PM_{2.5}$ in polluted days

3.3.1 Temporal evolution of $PM_{2.5}$ mass concentration in polluted days

Using the "Ambient Air Quality Standard" (GB3095-2012) of China (CAAQS), the occurrences of polluted days exceeding the daily threshold values during 2012-2014 were counted for each site (Fig. 6). Based on the number of polluted days exceeding the CAAQS daily guideline of 35 μg/m^3, substandard days of $PM_{2.5}$ account for more than 60% of the total period at the majority of urban sites, excepting Lhasa, Taipei and Sanya. Note that the ten most polluted cities (Ji'nan, Chengdu, Taiyuan, Hefei, Shenyang, Xi'an, Changsha, Shijiazhuang, Wuxi and Chongqing) experienced less than 20% clean days (daily $PM_{2.5}$<35 μg/m^3) during the three-year observation period. Interestingly, the occurrences of heavily polluted days (daily $PM_{2.5}$>150 μg/m^3) were different among these ten most polluted cities. While more than 15% of the total period comprised heavily polluted days in Ji'nan, Taiyuan, Chengdu, Xi'an and Shijiazhuang, heavily polluted days accounted for less than 5% of the total days in the other five cities, which mainly experienced slightly polluted (35-75 μg/m^3) and moderately polluted (75-115 μg/m^3) days. Due to the regional pollutant transports, the rural and background sites near the most polluted cities also showed high occurrences of polluted days. Polluted days accounted for more than 50% of the total period at Xin'long, Lin'an and Dinghu Mountain. In addition, an even higher occurrence of polluted days (>80%) was found for the rural areas of Yucheng and Xianghe. In contrast, the background sites in the TAR, NECR and SWCR rarely experienced polluted days, and over 80% of the total period comprised clean days at these sites.

The polluted days were not equally distributed throughout the year. The monthly distributions for the polluted days at each site are shown in Fig. 7. In terms of the occurrences of heavily polluted days, December, January and February were predominant months for the urban sites located in the

most polluted areas of the GZP and NCP, where both the unfavorable dispersion conditions for pollutants and the additional emission enhancements from residential heating contributed to the heavy pollution in the winter. The heavy pollution occurring in April and November in Cele was primarily caused by sandstorms and dust storms. Heavily polluted days were rarely observed at the 12 background sites in this study. The moderately polluted and polluted days were still mainly concentrated in the winter in the megacities of the GZP and NCP and also occurred in the winter in the megacities of the YRD and SWCR. In addition, March to June and September to October were periods with high occurrences of polluted days. Dust storms from northern China (March to April), biomass burning after crop harvests (May to June and September to October) and worsening dispersion conditions after the summers likely accounted for the polluted days (Cheng et al., 2014; Fu et al., 2014). The majority of slightly polluted days occurred from June to September, except at several urban sites in southern China. The mass level of 35-75 $\mu g/m^3$ was considered a low level of pollution for the entire year, illustrating that the summer and early autumn experienced cleaner conditions.

3.3.2 Chemical evolution of $PM_{2.5}$ composition in polluted days

The mean percentile compositions of the major components in $PM_{2.5}$ at different pollution levels from four paired urban-background sites are shown in Fig. 8. With the pollution level increased from clean to moderately polluted, the EC fraction in Beijing decreased slightly, the OM fraction decreased significantly, and the sulfate and nitrate contributions increased sharply (Fig. 8a). The same chemical evolution of the $PM_{2.5}$ was also observed at the background site of Xinglong, suggesting that regional transport plays a vital role in the formation of the slightly and moderately polluted days in the NCP. When the pollution level increased to heavily polluted, however, the OM fraction further increased and was accompanied by increases of the sulfate and nitrate contributions as well as decreases of the mineral dust contribution, indicating the enhanced secondary transformation of gaseous pollutants (etc. SO_2, NO*x*, VOCs) during heavily polluted periods (Liu et al., 2016a). Note that a steady increase of $[NO_3^-]/[SO_4^{2-}]$ ratio was observed with the aggravation of pollution (Fig. 8a), suggesting the relatively more important contribution of mobile than stationary sources (Arimoto et al., 1996). In addition, much higher OC/EC ratios were found in Beijing, especially during the heavily polluted days (OC/EC=6.3) (Fig. 8), compared with Guangzhou, Shenyang and Chongqing. Higher OC/EC ratio has been reported to be emitted from coal combustion (2.7) and biomass burning (6.6) than from motor vehicles (1.1) (Watson et al., 2001; Saarikoski et al., 2008). In the Northern China, the residential sector is the largest emitter of carbonaceous aerosols (Lei et al., 2011; Lu et al., 2011), which are formed by the inefficient combustion of fossil fuel and biomass in unregulated cooking and heating devices. For OC, the residential sector contribution can exceed 95% (Liu, et al., 2016c). Thus, the highest OC/EC ratio in Beijing indicates that residential emissions would also contributed considerably to the development of heavily polluted days.

Unlike in Beijing, the contributions of OM and EC were almost constant across the different pollution levels in Guangzhou, while the contribution of the secondary inorganic aerosols (SIA) increased slightly (Fig. 8b). Interestingly, the nitrate contribution increased faster than that of the sulfate when the pollution level increased from clean to heavily polluted, similar to the patterns of Beijing. Furthermore, the $[NO_3^-]/[SO_4^{2-}]$ ratio increased continuously and it reported the highest

ratio of $[NO_3^-]/[SO_4^{2-}]$ (1.3) during the heavily polluted days in Guangzhou (Fig. 8). At the same time, the ratio of OC/EC was nearly constant with the aggravation of pollution, and it reported the lowest OC/EC ratio (1.6-1.8) among the four megacities. These results suggest the dominate contribution of local traffic emissions in the development of fine particulate pollution. The chemical evolution of $PM_{2.5}$ at the background site of PRD was similar to that of the urban site at Guangzhou, although a significant contribution of SIA was observed when the pollution level increased from clean to moderately polluted (34% vs. 58%). Note that the contribution of sulfate increased sharply, suggesting that regional transports dominated the particle pollution during heavily polluted days.

Compared with Beijing, a reversed chemical evolution of $PM_{2.5}$ for the different pollution levels was observed in Shenyang, with the OM fraction increasing sharply from 22% to 37%, while the SIA decreased slightly from 39% to 31% (Fig. 8c). Note that a steady increase of sulfate from slightly polluted days to heavily polluted days was observed. In addition, a nearly constant low ratio of $[NO_3^-]/[SO_4^{2-}]$ (0.30-0.38) and continually increased ratio of OC/EC (2.3-4.5) was observed with the aggravation of pollution. These results suggest that enhanced local stationary emissions like coal combustion dominate the temporal evolution of $PM_{2.5}$ on polluted days in Shenyang. The highest concentration of Cl^- in Shenyang than other cities in this study further support the significant contribution of coal combustion. A similar chemical evolution of $PM_{2.5}$ was found at the background site of Changbai Mountain, which showed a significantly increased OM fraction and slightly decrease of SIA when the pollution level increased from clean to slighted polluted, indicating the enhanced contribution from local emissions like coal combustion for heating during slightly polluted days. Further support for this pattern is seen in the increase of the EC fraction (Fig. 8 g).

Similar to that in Guangzhou, the contribution of OM was almost constant for different pollution levels in Chongqing, while much higher contribution of SIA was observed, especially during the heavily polluted days. In addition, a steady increase of $[NO_3^-]/[SO_4^{2-}]$ ratio was observed, similar with those in Beijing and Guangzhou, suggesting the relatively more important contribution of mobile than stationary sources (Arimoto et al., 1996). Furthermore, the OC/EC ratio was also continually increased with the aggravation of pollution, and different from that in Guangzhou but similar with that in Shenyang. Note that the fraction of OM, sulfate and nitrate during the heavily polluted days in Chongqing was much higher than those in Beijing, Guangzhou and Shenyang, suggesting the higher oxidation capacity and therefore higher formation efficiency from gaseous pollutants (etc. SO_2, NO*x*, VOCs) to secondary aerosol. These results suggest the importance of local traffic emissions and the formation of secondary aerosol in driving $PM_{2.5}$ pollution in Chongqing. The background site of Gongga Mountain shows decreased contributions of OM, EC, SIA and mineral dust when the pollution level increased from clean to slightly polluted days, similar to the pattern observed in Xinglong. Note that the unaccounted-for fraction was largely increased on slightly polluted days (33% vs. 10%), possibly due to the increase of aerosol-bound water related to the hygroscopic growth of aerosols at high RH values on slightly polluted days (Bian et al., 2014).

4. Conclusions

We have established a national-level network ("Campaign on atmospheric Aerosol REsearch" network of China (CARE-China)) that conducted continuous monitoring of $PM_{2.5}$ mass concentrations at 40 ground observation station, including 20 urban sites, 12 background sites and 8 rural/suburban sites. The average aerosol chemical composition was inferred from the filter

samples from six paired urban and background sites, which represent the largest megacities and regional background areas in the five most polluted regions and the TAR of China. This study presents the first long-term dataset including three-year observations of online $PM_{2.5}$ mass concentrations (2012-2014) and one year observations of $PM_{2.5}$ compositions (2012-2013) from the CARE-China network. One of the major purposes of this study was to compare and contrast urban and background aerosol concentrations from nearby regions. The major findings include the following:

(1) The average $PM_{2.5}$ concentration from 20 urban sites is 73.2 $\mu g/m^3$ (16.8-126.9 $\mu g/m^3$), which is three times greater than the average value of 12 background sites (11.2-46.5 $\mu g/m^3$). The highest $PM_{2.5}$ concentrations were observed at the stations on the Guanzhong Plain (GZP) and the NCP. The $PM_{2.5}$ pollution is also a serious problem for the industrial regions of northeastern China and the Sichuan Basin and is a relatively less serious problem for the YRD and the PRD. The background $PM_{2.5}$ concentrations of the NCP, YRD and PRD were comparable to those of the nearby urban sites, especially for the PRD. A distinct seasonal variability of the $PM_{2.5}$ is observed, presenting peaks during the winter and minima during the summer at the urban sites, while the seasonal variations of $PM_{2.5}$ at the background sites vary in different part of China. Bimodal and unimodal diurnal variation patterns were identified at both the urban and background stations.

(2) The major $PM_{2.5}$ constituents across all the urban sites are OM (26.0%), SO_4^{2-}(17.7%), mineral dust (11.8%), NO_3^- (9.8%), NH_4^+ (6.6%), EC (6.0%), Cl^- (1.2%) at 45% RH and unaccounted matter (20.7%). Similar chemical compositions of $PM_{2.5}$ were observed for the background sites and were associated with higher fractions of OM (33.2%) and lower fractions of NO_3^- (8.6%) and EC (4.1%). Analysis of filter samples reveals that several $PM_{2.5}$ chemical components varied by more than an order of magnitude between sites. For urban sites, the OM ranges from 12.6 $\mu g/m^3$ (Lhasa) to 23.3 $\mu g/m^3$ (Shenyang), the SO_4^{2-} ranges from 0.8 $\mu g/m^3$ (Lhasa) to 19.7 $\mu g/m^3$ (Chongqing), the NO_3^- ranges from 0.5 $\mu g/m^3$ (Lhasa) to 11.9 $\mu g/m^3$ (Shanghai) and the EC ranges from 1.4 $\mu g/m^3$ (Lhasa) to 7.1 $\mu g/m^3$ (Guangzhou). The $PM_{2.5}$ chemical species of the background sites exhibit larger spatial heterogeneities than those of the urban sites, suggesting the different contributions from regional anthropogenic and natural emissions and from the long-range transport to background areas.

(3) Notable seasonal variations of $PM_{2.5}$ polluted days were observed, especially for the megacities in east-central China, resulting in frequent heavy pollution episodes occurring during the winter. The increasing contribution of secondary aerosol on polluted days was observed both for the urban and nearby background sites, suggesting fine particle pollution in the most polluted areas of China assumes a regional tendency, and the importance to address the emission reduction of secondary aerosol precursors. In addition, the chemical species dominating the evolutions of the heavily polluted events were different, while decreasing or constantly contribution of OM associated with increasing contribution of SIA characteristic evolution of $PM_{2.5}$ in NCP, PRD and SWCR, the opposite phenomenon was observed in NECR. Further analysis from the $[NO_3^-]/[SO_4^{2-}]$ ratio and OC/EC ratio showed that fine particle pollution in Guangzhou and Shenyang was mainly attributed to the traffic emissions and coal combustion, respectively, while more complex and variable major sources including mobile vehicle emission and residential sources contributed to the development of heavily polluted days in Beijing. As for Chongqing, the higher oxidation capacity than other cities

suggested it should pay more attention to the emission reduction of secondary aerosol precursors. These results suggest the different formation mechanisms of the heavy pollution in the most polluted city clusters, and unique mitigation measures should be developed for the different regions of China.

The seasonal and spatial patterns of urban and background aerosols emphasize the importance of understanding the variabilities of the concentrations of major aerosol species and their contributions to the $PM_{2.5}$ budget. Comparisons of $PM_{2.5}$ chemical compositions from urban and background sites of adjacent regions provided meaningful insights into aerosol sources and transport and into the role of urban influences on nearby rural regions. The integration of data from 40 sites from the CARE-China network provided an extensive spatial coverage of fine particle concentrations near the surface and could be used to validate model results and implement effective air pollution control strategies.

Acknowledgments

This study was supported by the Ministry of Science and Technology of China (Grant nos. 2017YFC0210000), the National Natural Science Foundation of China (Grant nos. 41705110) and the Strategic Priority Research Program of the Chinese Academy of Sciences (Grant nos. XDB05020200 & XDA05100100). We acknowledge the tremendous efforts of all the scientists and technicians involved in the many aspects of the Campaign on atmospheric Aerosol REsearch network of China (CARE-China).

References

Arimoto, R., Duce, R. A., Savoie, D. L., Prospero, J., Talbot, R., Cullen, J., Tomza, U., Lewis, N., and Ray, B.: Relationships among aerosol constituents from Asia and the North Pacific during PEM-West A, J. Geophys. Res., 101, 2011-2023, 1996.

Bell, M. L., Dominici, F., Ebisu, K., Zeger, S. L., and Samet, J. M.: Spatial and temporal variation in $PM_{2.5}$ chemical composition in the United States for health effects studies. Environ Health Perspect., 115, 989-995, 2007.

Bian, Y. X., Zhao, C. S., Ma, N., Chen, J., and Xu, W. Y.: A study of aerosol liquid water content based on hygroscopicity measurements at high relative humidity in the North China Plain. Atmos. Chem. Phys., 14, 6417-6426, 2014.

Boyouk, N., Léon, J. F., Delbarre, H., Podvin, T., and Deroo, C.: Impact of the mixing boundary layer on the relationship between $PM_{2.5}$ and aerosol optical thickness. Atmos. Environ., 44(2), 271-277, 2010.

Chan, C. K., and Yao X. H.: Air pollution in mega cities in China. Atmos. Environ., 42(1), 1-42, 2008.

Chen, W. H., Wang, X. M., Zhou, S. Z., Cohen, J. B., Zhang, J., Wang, Y., Chang, M., Zeng, Y., Liu, Y., Ling, Z., Liang, G., and Qiu, X.: Chemical Composition of $PM_{2.5}$ and its Impact on Visibility in Guangzhou, Southern China. Aerosol Air Qual. Res., 16, 2349-2361, 2016.

Chen, Y., Xie, S. D., Luo, B., and Zhai, C. Z.: Particulate pollution in urban Chongqing of southwest China: Historical trends of variation, chemical characteristics and source apportionment. Sci. Total Environ., 584-585, 523-534, 2017.

Chen, Z., Wang, J. N., Ma, G. X., and Zhang, Y. S.: China tackles the health effects of air pollution. Lancet, 382, 1959-1960, 2013.

Cheng, Z., Wang, S., Fu, X., Watson, J. G., Jiang, J., Fu, Q., Chen, C., Xu, B., Yu, J., Chow, J. C., and Hao, J.: Impact of biomass burning on haze pollution in the Yangtze River delta, China: a case study in summer 2011. Atmos. Chem.

Phys., 14 (9), 4573-4585, 2014.
Cheng, Z., Luo, L., Wang, S., Wang, Y., Sharma, S., Shimadera, H., Wang, X., Bressi, M., Maura de Miranda, R., Jiang, J., Zhou, W., Fajardo, O., Yan, N., Hao, J.: Status and characteristics of ambient $PM_{2.5}$ pollution in global megacities. Environ. Int., 89-90, 212-221, 2016.
Cong, Z., Kang, S., Luo, C., Li, Q., Huang, J., Gao, S. P., and Li, X. D.: Trace elements and lead isotopic composition of PM_{10} in Lhasa, Tibet. Atmos. Environ., 45, 6210-6215, 2011.
Cusack, M., Alastuey, A., P´erez, N., Pey, J., and Querol, X.: Trends of particulate matter ($PM_{2.5}$) and chemical composition at a regional background site in the Western Mediterranean over the last nine years (2002–2010). Atmos. Chem. Phys., 12, 8341-8357, 2012.
Dickerson, R.R., Li, C., Li, Z., Marufu, L.T., Stehr, J.W., McClure, B., Krotkov, N., Chen, H., Wang, P., Xia, X., Ban, X., Gong, F., Yuan, J., and Yang, J.: Aircraft observations of dust and pollutants over northeast China: insight into the meteorological mechanisms of transport. J. Geophys. Res., 112, D24S90, doi: 10.1029/2007JD008999, 2007.
Eeftens, M., Tsai, M.-Y., Ampe, C., Anwander, B., Beelen, R., Bellander, T., Cesaroni, G., Cirach, M., Cyrys, J., Hoogh, K. D., Nazelle, A. D., Vocht, F. D., Declercq, C., Dedele, A., Eriksen, K., Galassi, C., Grazuleviciene, R., Grivas, G., Heinrich, J., Hoffmann, B., Iakovides, M., Ineichen, A., Katsouyanni, K., Korek, M., Krämer, U., Kuhlbusch, T., Lanki, T., Madsen, C., Meliefste, K., Mölter, A., Moslerm, G., Nieuwenhuijsen, M., Oldenwening, M., Pennanen, A., Probst-Hensch, N., Quass, U., Raaschou-Nielsen, O., Ranzi, A., Stephanou, E., Sugiri, D., Udvardy, O., Vaskövi, É., Weinmayr, G., Brunekreef, B., and Hoek, G.: Spatial variation of $PM_{2.5}$, PM_{10}, $PM_{2.5}$ absorbance and PM coarse concentrations between and within 20 European study areas and the relationship with NO_2 - Results of the ESCAPE project. Atmos. Environ., 62, 303-317, 2012.
Fu, X., Wang, S. X., Zhao, B., Xing, J., Cheng, Z., Liu, H., and Hao, J. M.: Emission inventory of primary pollutants and chemical speciation in 2010 for the Yangtze River Delta region, China. Atmos. Environ., 70, 39-50, 2013.
Fu, X., Wang, S. X., Cheng, Z., Xing, J., Zhao, B., Wang, J. D., and Hao, J. M.: Source, transport and impacts of a heavy dust event in the Yangtze River Delta, China, in 2011. Atmos. Chem. Phys., 14 (3), 1239-1254, 2014.
Gehrig, R., and Buchmann, B.: Characterising seasonal variations and spatial distribution of ambient PM_{10} and $PM_{2.5}$ concentrations based on long-term Swiss monitoring data. Atmos. Environ., 37, 2571-2580, 2003.
Guo, S., Hu, M., Zamora, M. L., Peng, J., Shang, D., Zheng, J., Du, Z., Wu, Z., Shao, M., Zeng, L., Molina, M. J., and Zhang, R.: Elucidating severe urban haze formation in China. Proc. Nat. Acad. Sci. U.S.A. 111, 17373-17378, 2014.
Hand, J. L., Schichtel, B. A., Pitchford, M., Malm, W. C., and Frank, N. H.: Seasonal composition of remote and urban fine particulate matter in the United States. J. Geophys. Res., 117, D05209, doi: 10.1029/2011JD017122, 2012.
He, K. B., Yang, F. M., Ma, Y. L., Zhang, Q., Yao, X. H., Chan, C. K., Cadle, S., Chan, T., and Mulawa, P.: The characteristics of $PM_{2.5}$ in Beijing, China. Atmos. Environ., 35(29), 4959-4970, 2001.
Hoffer, A., Gelencser´, A., Guyon, P., Kiss, G., Schmid, O., Frank, G. P., Artaxo, P. and Andreae, M. O.: Optical properties of humic-like substances (HULIS) in biomass-burning aerosols. Atmos. Chem. Phys., 6, 3563-3570, 2006.
Huang, R. J., Zhang, Y., Bozzetti, C., Ho, K., Cao, J., Han, Y., Daellenbach, K., Slowik, J., Platt, S., Canonaco, F., Zotter, P., Wolf, R., Pieber, S., Bruns, E., Crippa, M., Ciarelli, G., Piazzalunga, A., Schwikowski, M., Abbaszade, G., Schnelle-Kreis, J., Zimmermann, R., An, Z., Szidat, S., Baltensperger, U., Haddad, I., and Prévôt, A.: High secondary aerosol contribution to particulate pollution during haze events in China. Nature, 514, 218-222, 2014.
Huang, Y., Li, L., Li, J., Wang, X., Chen, H., Chen, J., Yang, X., Gross, D. S., Wang, H., Qiao, L., and Chen, C.: A case study of the highly time-resolved evolution of aerosol chemical and optical properties in urban Shanghai, China. Atmos. Chem. Phys., 13(8), 3931-3944, 2013.

IPCC: Climate Change 2013: The Physical Science Basis: Summary for Policymakers, Cambridge, UK, 2013.

Janssen, N. A. H., Fischer, P., Marra, M., Ameling, C., and Cassee, F. R.: Short-term effects of $PM_{2.5}$, PM_{10} and $PM_{2.5-10}$ on daily mortality in the Netherlands. Sci. Total. Environ., 463-464, 20-26, 2013.

Lei, Y., Zhang, Q., He, K. B., Streets, D. G.: Primary anthropogenic aerosol emission trends for China, 1990-2005. Atmos. Chem. Phys., 11(3), 931-954, 2011.

Li, L., Chen, C. H., Fu, J. S., Huang, C., Streets, D. G., Huang, H. Y., Zhang, G. F., Wang, Y. J., Jang, C. J., Wang, H. L., Chen, Y. R., and Fu. J. M.: Air quality and emissions in the Yangtze River Delta, China. Atmos. Chem. Phys., 11, 1621-1639, 2011

Li, Y. C., Yu, J. Z., Ho, S. S. H., Yuan, Z. B., Lau, A. K. H., and Huang X. F.: Chemical characteristics of $PM_{2.5}$ and organic aerosol source analysis during cold front episodes in Hong Kong, China. Atmos. Res., 118, 41-51, 2012.

Liu, Z. R., Hu, B., Wang, L. L., Wu, F. K., Gao, W. K., and Wang, Y. S.: Seasonal and diurnal variation in particulate matter (PM_{10} and $PM_{2.5}$) at an urban site of Beijing: analyses from a 9-year study. Environ. Sci. Pollut. Res., 22, 627-642, 2015.

Liu, L., Zhang, X., Wang, S., Zhang, W., and Lu, X.: Bulk sulfur (S) deposition in China. Atmos. Environ., 135, 41-49, 2016b.

Liu, J., Mauzerall, D. L., Chen, Q., Zhang, Q., Song, Y., Peng, W., Klimont, Z., Qiu, X., Zhang, S., Hu, M., Lin, W., Smith, K. R., and Zhu, Tong.: Air pollutant emissions from Chinese households: A major and underappreciated ambient pollution source. PANS, 113(28), 7756-7761, 2016c.

Liu, Z. R., Wang, Y. S., Hu, B., Ji, D. S., Zhang, J. K., Wu, F. K., Wan, X. and Wang, Y. H.: Source appointment of fine particle number and volume concentration during severe haze pollution in Beijing in January 2013. Environ. Sci. Pollut. Res., 23(7), 6845-6860, 2016a.

Liu, Z. R., Wang, Y. S., Liu, Q., Liu, L. N., and Zhang, D. Q.: Pollution Characteristics and Source of the Atmospheric Fine Particles and Secondary Inorganic Compounds at Mount Dinghu in Autumn Season (in Chinese). Environ. Sci., 32, 3160-3166, 2011.

Liu, Z. R., Xie, Y., Hu, B., Wen, T., Xin, J., Li, X., Wang, Y. S.: Size-resolved aerosol water-soluble ions during the summer and winter seasons in Beijing: Formation mechanisms of secondary inorganic aerosols. Chemosphere, 183, 119-131, 2017.

Lu, Z., Streets, D. G., Zhang, Q., Wang, S., Carmichael, G. R., Cheng, Y. F., Wei, C., Chin, M., Dieh, T., and Tan, Q.: Sulfur dioxide emissions in China and sulfur trends in East Asia since 2000. Atmos. Chem. Phys., 10, 6311-6331, 2010.

Lu, Z., Zhang, Q., Streets, D. G.: Sulfur dioxide and primary carbonaceous aerosol emissions in China and India, 1996-2010. Atmos. Chem. Phys., 11(18), 9839-9864, 2011.

Malm, W. C., Schichtel, B. A., Pitchford, M. L., Ashbaugh, L. L., and Eldred, R. A.: Spatial and monthly trends in speciated fine particle concentration in the United States. J. Geophys. Res., 109, D03306, doi: 10.1029/2003JD003739, 2004.

Mamtimin, B., and Meixner, F. X.: Air pollution and meteorological processes in the growing dryland city of Urumqi (Xinjiang, China). Sci. Total Environ., 409(7), 1277-1290, 2011.

Mao, Y. H., Liao, H., and Chen, H. S.: Impacts of East Asian summer and winter monsoons on interannual variations of mass concentrations and direct radiative forcing of black carbon over eastern China. Atmos. Chem. Phys., 17, 4799-4816, 2017.

Mason, B.: Principles of Geochemistry, New York, Wiley, 1966.

Mauderly, J. L., and Chow, J. C.: Heath effects of organic aerosols. Inhal. Toxicol., 20, 257-288, 2008.

Niu, Z. C., Zhang, F. W., Chen, J. S., Yin, L. Q., Wang, S., and Xu, L. L.: Carbonaceous species in $PM_{2.5}$ in the coastal urban agglomeration in the Western Taiwan Strait Region, China. Atmos. Res., 122, 102-110, 2013.

Oanh, N. T. K., Upadhyay, N., Zhuang, Y. H., Hao, Z. P., Murthy, D. V. S., Lestari, P., Villarin, J. T., Chengchua, K., Co, H. X., Dung, N. T., and Lindgren, E. S.: Particulate air pollution in six Asian cities: Spatial and temporal distributions, and associated sources. Atmos. Environ., 40, 3367-3380, 2006.

Pan, Y. P., Wang, Y. S., Sun, Y., Tian, S. L., and Cheng, M. T.: Size-resolved aerosol trace elements at a rural mountainous site in Northern China: Importance of regional transport. Sci. Total Environ., 461, 761-771, 2013.

Patashnick, H., and Rupprecht, E.: Continuous PM_{10} measurements using the tapered element oscillating microbalance. J. Air Waste Manage., 41, 1079-1083, 1991.

Putaud, J. P., Van Dingenen, R., Alastuey, A., Bauer, H., Birmili, W., Cyrys, J., Flentje, H., Fuzzi, S., Gehrig, R., Hansson, H. C., Harrison, R. M., Herrmann, H., Hitzenberger, R., Hüglin, C., Jones, A. M., Kasper-Giebl, A., Kiss, G., Kousa, A., Kuhlbusch, T. A. J., Löschau, G., Maenhaut, W., Molnar, A., Moreno, T., Pekkanen, J., Perrino, C., Pitz, M., Puxbaum, H., Querol, X., Rodriguez, S., Salma, I., Schwarz, J., Smolik, J., Schneider, J., Spindler, G., ten Brink, H., Tursic, J., Viana, M., Wiedensohler, A., and Raes, F.: A European aerosol phenomenology - 3: Physical and chemical characteristics of particulate matter from 60 rural, urban, and kerbside sites across Europe. Atmos. Environ., 44, 1308-1320, 2010.

Quan, J. N., Tie, X. X., Zhang, Q., Liu, Q., Li, X., Gao, Y., and Zhao, D. L.: Characteristics of heavy aerosol pollution during the 2012-2013 winter in Beijing, China. Atmos. Environ., 88, 83-89, 2014.

Saarikoski, S., Timonen, H., Saarnio, K., Aurela, M., Järvi, L., Keronen, P., Kerminen, V.-M., and Hillamo, R.: Sources of organic carbon in fine particulate matter in northern European urban air, Atmos. Chem. Phys., 8, 6281-6295, https://doi.org/10.5194/acp-8-6281-2008, 2008.

Seinfeld, J. H., and Pandis, S. N.: Atmospheric Chemistry and Physics: from Air Pollution to Climate Change. Wiley, New York, USA, 2016.

Sun, Q. H., Hong, X. R., and Wold, L. E.: Cardiovascular Effects of Ambient Particulate Air Pollution Exposure. Circulation, 121(25), 2755-2765, 2010.

Tao, J., Zhang, L. M., Ho, K. F., Zhang, R. J., Lin, Z. J., Zhang, Z. S., Lin, M., Cao, J. J., Liu, S. X., and Wang, G. H.: Impact of $PM_{2.5}$ chemical compositions on aerosol light scattering in Guangzhou - the largest megacity in South China. Atmos. Res., 135, 48-58, 2014.

Tao, J., Zhang, L. M., Cao, J. J., Zhong, L. J., Chen, D. S., Yang, Y. H., Chen, D. H., Chen, L. G., Zhang, Z. S., Wu, Y. F., Xia, Y. J., Ye, S. Q., and Zhang, R. J.: Source apportionment of $PM_{2.5}$ at urban and suburban areas of the Pearl River Delta region, south China - With emphasis on ship emissions. Sci. Total Environ., 574, 1559-1570, 2017.

Turpin, B. J., and Lim, H. J.: Species contributions to $PM_{2.5}$ mass concentrations: Revisiting common assumptions for estimating organic mass. Aerosol Sci. Technol., 35, 602-610, 2001.

Verma, R. L., Sahu, L. K., Kondo, Y., Takegawa, N., Han, S., Jung, J. S., Kim, Y. J., Fan, S., Sugimoto, N., Shammaa, M. H., Zhang, Y. H., and Zhao, Y.: Temporal variations of black carbon in Guangzhou, China, in summer 2006. Atmos. Chem. Phys., 10, 6471-6485, 2010.

Viana, M., X., Querol, A., Alastuey, F., Ballester, S., Llop, A., Esplugues, R., Fernandez-Patier, S., dos Santos, G., and Herce, M. D.: Characterising exposure to PM aerosols for an epidemiological study. Atmos. Environ., 42(7), 1552-1568, 2008.

Wan, X., Kang, S. C., Xin, J. Y., Liu, B., Wen, T. X., Wang, P. L., Wang, Y. S., and Cong, Z. Y.: Chemical composition of size-segregated aerosols in Lhasa city, Tibetan Plateau. Atmos. Res., 174-175, 142-150, 2016.

Wang, Y. S., Yao, L., Wang, L. L., Liu, Z. R., Ji, D. S., Tang, G. Q., Zhang, J. K., Sun, Y., Hu, B., and Xin, J. Y.:

Mechanism for the formation of the January 2013 heavy haze pollution episode over central and eastern China. Sci. China: Earth Sci., 57, 14-25, 2014.

Wang, G. H., Zhou, B. H., Cheng, C. L., Cao, J. J., Li, J. J., Meng, J. J., Tao, J., Zhang, R. J., and Fu, P. Q.: Impact of Gobi desert dust on aerosol chemistry of Xi'an, inland China during spring 2009: differences in composition and size distribution between the urban ground surface and the mountain atmosphere. Atmos. Chem. Phys., 13(2), 819-835, 2013.

Wang, H. B., Tian, M., Li, X., Chang, Q., Cao, J., Yang, F., Ma, Y., He, K.: Chemical Composition and Light Extinction Contribution of $PM_{2.5}$ in Urban Beijing for a 1-Year Period. Aerosol and Air Quality Research, 15, 2200-2211, 2015a.

Wang, H. L., Qiao, L. P., Lou, S. R., Zhou, M., Ding, A. J., Huang, H. Y., Chen, J. M., Wang, Q., Tao, S. K., Chen, C. H., Li, L., and Huang, C.: Chemical composition of $PM_{2.5}$ and meteorological impact among three years in urban Shanghai, China. J. Clean. Prod., 112, 1302-1311, 2016.

Wang, Y. Q., Zhang, X. Y., Sun, J. Y., Zhang, X. C., Che, H. Z., and Li, Y.: Spatial and temporal variations of the concentrations of PM_{10}, $PM_{2.5}$ and PM_1 in China. Atmos. Chem. Phys., 15, 13585-13598, 2015b.

Watson, J. G., Chow, J. C., and Houck, J. E.: $PM_{2.5}$ chemical source profiles for vehicle exhaust, vegetative burning, geological material, and coal burning in Northwestern Colorado during 1995, Chemosphere, 43, 1141-1151, https://doi.org/10.1016/S0045-6535(00)00171-5, 2001.

Westerdahl, D., Wang, X., Pan, X. C. and Zhang, K. M.: Characterization of on-road vehicle emission factors and microenvironmental air quality in Beijing, China. Atmos. Environ. 43, 697-705, 2009.

Wu, F. K., Yu, Y., Sun, J., Zhang, J. K., Wang, J., Tang, G. Q., and Wang, Y. S.: Characteristics, source apportionment and reactivity of ambient volatile organic compounds at Dinghu Mountain in Guangdong Province, China. Sci. Total Environ., 548-549, 347-359, 2016.

Xia, X. A., Chen, H. B., Wang, P. C., Zhang, W. X., Goloub, P., Chatenet, B., Eck, T. F., and Holben, B. N.: Variation of column-integrated aerosol properties in a Chinese urban region. J. Geophys. Res.-Atmos., 111, D05204, doi: 10.1029/2005JD006203, 2006.

Xin, J., Wang, Y., Pan, Y., Ji, D., Liu, Z., Wen, T., Wang, Y., Li, X., Sun, Y., Sun, J., Wang, P., Wang, G., Wang, M., Cong, Z., Song, T., Hu, B., Wang, L., Tang, G., Gao, W., Guo, Y., Miao, H., Tian, S., and Wang, L.: The Campaign on atmospheric Aerosol REsearch network of China: CARE-China. BAMS, 96(7), 1137-1155, 2015.

Xing, L., Fu, T. M., Cao, J. J., Lee, S. C., Wang, G. H., Ho, K. F., Cheng, M. C., You, C. F., and Wang, T. J.: Seasonal and spatial variability of the OM/OC mass ratios and high regional correlation between oxalic acid and zinc in Chinese urban organic aerosols. Atmos. Chem. Phys., 13, 4307-4318, 2013.

Xu, J. S., Xu, M. X., Snape, C., He, J., Behera, S. N., Xu, H. H., Ji, D. S., Wang, C. J., Yu, H., Xiao, H., Jiang, Y. J., Qi, B., and Du, R. G.: Temporal and spatial variation in major ion chemistry and source identification of secondary inorganic aerosols in Northern Zhejiang Province, China. Chemosphere, 179, 316-330, 2017.

Yang, F., Tan, J., Zhao, Q., Du, Z., He, K., Ma, Y., Duan, F., and Chen, G.: Characteristics of $PM_{2.5}$ speciation in representative megacities and across China. Atmos. Chem. Phys., 11(11), 5207-5219, 2011.

Yang Y. J., Wang Y. S, Wen T. X, Li, W., Zhao, Y., Li L.: Elemental composition of $PM_{2.5}$ and PM_{10} at Mount Gongga in China during 2006. Atmos. Res. 93, 801-810, 2009.

Ye, B., Ji, X., Yang, H., Yao, X., Chan, C. K., Cadle, S. H., Chan, T., and Mulawa, P. A.: Concentration and chemical composition of $PM_{2.5}$ in Shanghai for a 1-year period. Atmos. Environ., 37, 499-510, 2003.

Zhang, C., Zhou, R., and Yang, S.: Implementation of clean coal technology for energy-saving and emission reduction in Chongqing. Environment and Ecology in the Three Gorges (in Chinese), 3, 52-56, 2010.

Zhang, J. K., Sun, Y., Wu, F. K., Sun, J., and Wang, Y. S.: The characteristics, seasonal variation and source apportionment of VOCs at Gongga Mountain, China. Atmos. Environ., 88, 297-305, 2014c.

Zhang, L. W., Chen, X., Xue, X. D., Sun, M., Han, B., Li, C. P., Ma, J., Yu, H., Sun, Z. R., Zhao, L. J., Zhao, B. X., Liu, Y. M., Chen, J., Wang, P. P., Bai, Z. P., and Tang, N. J.: Long-term exposure to high particulate matter pollution and cardiovascular mortality: A 12-year cohort study in four cities in northern China. Environ. Int., 62, 41-47, 2014a.

Zhang, N. N., Cao, J. J., Liu, S. X., Zhao, Z. Z., Xu, H. M., and Xiao, S.: Chemical composition and sources of $PM_{2.5}$ and TSP collected at Qinghai Lake during summertime. Atmos. Res., 138, 213-222, 2014b.

Zhang, X. Y., Wang, Y. Q., Niu, T., Zhang, X. C., Gong, S. L., Zhang, Y. M., and Sun, J. Y.: Atmospheric aerosol compositions in China: spatial/temporal variability, chemical signature, regional haze distribution and comparisons with global aerosols. Atmos. Chem. Phys. 12 (2), 779-799, 2012.

Zhang, Y. L., and Cao, F.: Fine particulate matter ($PM_{2.5}$) in China at a city level. Sci. Rep., 5: 14884. 2015.

Zhao, M. F., Huang, Z. S., Qiao, T., Zhang, Y. K., Xiu, G. L., and Yu, J. Z.: Chemical characterization, the transport pathways and potential sources of $PM_{2.5}$ in Shanghai: seasonal variations. Atmos. Res., 158, 66-78, 2015.

Zhao, P. S., Dong, F., Yang, Y. D., He, D., Zhao, X. J., Zhang, W. Z., Yao, Q., and Liu, H. Y.: Characteristics of carbonaceous aerosol in the region of Beijing, Tianjin, and Hebei, China. Atmos. Environ., 71, 389-398, 2013a.

Zhao, X. J., Zhao, P. S., Xu, J., Meng, W., Pu, W. W., Dong, F., He, D., and Shi, Q. F.: Analysis of a winter regional haze event and its formation mechanism in the North China Plain. Atmos. Chem. Phys., 13(11), 5685-5696, 2013b.

Zheng, J., Zhang, L., Che, W., Zheng, Z., and Yin, S.: A highly resolved temporal and spatial air pollutant emission inventory for the Pearl River Delta region, China and its uncertainty assessment. Atmos. Environ. 43, 5112-5122, 2009.

Zhou, S. Z., Wang, Z., Gao, R., Xue, L., Yuan, C., Wang, T., Gao, X., Wang, X., Nie, W., Xu, Z., Zhang, Q., and Wang, W.: Formation of secondary organic carbon and long-range transport of carbonaceous aerosols at Mount Heng in South China. Atmos. Environ., 63, 203-212, 2012.

Zhu, K., Zhang, J., Lioy, P. J.: Evaluation and Comparison of Continuous Fine Particulate Matter Monitors for Measurement of Ambient Aerosols, J. Air & Waste Manage. Assoc., 57:12, 1499-1506, 2007.

Zimmermann, R.: Aerosols and health: a challenge for chemical and biological analysis. Anal Bioanal Chem., 407, 5863-5867, 2015.

Zou, X. K., and Zhai, P. M.: Relationship between vegetation coverage and spring dust storms over northern China. J. Geophys. Res., 109, D03104, doi: 10.1029/2003JD003913, 2004.

1081 Table 1 Geographic information and three-year mean $PM_{2.5}$ concentration of the monitor stations.

Station/Code	Latitude, Longitude	Altitude(m)	Station type	Mean(μg/m3)	N(day)
Beijing/BJC	39.97°N, 116.37°E	45	Northern city	69.4±54.8	1077
Cele/CLD	37.00°N, 80.72°E	1306	Northwestern country	126.9±155.4	600
Changbai Mountain/CBM	42.40°N, 128.01°E	738	Northeastern background	17.6±12.6	807
Changsha/CSC	28.21°N, 113.06°E	45	Central city	77.9±45.4	1045
Chengdu/CDC	30.67°N, 104.06°E	506	Southwestern city	102.2±66.2	1008
Chongqing/CQC	29.59°N, 106.54°E	259	Southwestern city	65.1±35.8	972
Dinghu Mountain/DHM	23.17°N, 112.50°E	90	Pearl River Delta background	40.1±25.0	954
Dunhuang/DHD	40.13°N, 94.71°E	1139	Desert town	86.2±94.3	726
Fukang/FKZ	44.28°N, 87.92°E	460	Northwestern country	69.9±69.6	960
Gongga Mountain/GGM	29.51°N, 101.98°E	1640	Southwestern background	25.5±15.5	869
Guangzhou/GZC	23.16°N, 113.23°E	43	Southern city	44.1±23.8	772
Hailun/HLA	47.43°N, 126.63°E	236	Northeastern country	41.6±45.0	1076
Hefei/HFC	31.86°N, 117.27°E	24	Eastern city	80.4±45.3	909
Ji'nan/JNC	36.65°N, 117.00°E	70	Northern city	107.8±57.4	701
Kunming/KMC	25.04°N, 102.73°E	1895	Southwestern city	47.0±25.2	967
Lhasa/LSZ	29.67°N, 91.33°E	3700	Tibet city	30.6±21.3	600
Lin'an/LAZ	30.30°N, 119.73°E	139	Eastern background	46.5±27.2	1086
Mount Everest/ZFM	28.21°N, 86.56°E	4700	Tibet background	24.4±25.1	390
Namtso/NMT	30.77°N, 90.98°E	4700	Tibet background	11.2±6.9	499
Nagri/ALZ	32.52°N, 79.89°E	4300	Tibet background	19.5±12.4	72
Qianyanzhou/QYZ	26.75°N, 115.07°E	76	Southeastern country	52.1±28.4	927
Qinghai Lake/QHL	37.62°N, 101.32°E	3280	Tibet background	16.2±17.0	590
Sanya/SYB	18.22°N, 109.47°E	8	Southern island city	16.8±13.1	595
Shanghai/SHC	31.22°N, 121.48°E	9	Eastern city	56.2±59.4	822
Shapotou/SPD	37.45°N, 104.95°E	1350	Desert background	51.1±33.3	1016
Shenyang/SYC	41.50°N, 123.40°E	49	Northeastern city	77.6±41.2	926
Shijiazhuang/SJZ	38.03°N, 114.53°E	70	Northern city	105.1±92.7	1031
Taipei/TBC	25.03°N, 121.90°E	150	Island city	22.1±10.7	1083
Taiyuan/TYC	37.87°N, 112.53°E	784	Northern city	111.5±74.9	987
Tianjin/TJC	39.08°N, 117.21°E	9	Northern city	69.9±49.6	1034
Tongyu/TYZ	44.42°N, 122.87°E	160	Inner Mongolia background	24.5±24.5	757
Urumchi/URC	43.77°N, 87.68°E	918	Northwestern city	104.1±145.2	776
Wuxi/WXC	31.50°N, 120.35°E	5	Eastern city	65.2±36.8	1003
Xi'An/XAC	34.27°N, 108.95°E	397	Central city	125.8±108.2	1077
Xianghe/XHZ	39.76°N, 116.95°E	25	North China suburbs	83.7±62.3	1084
Xinglong/XLZ	40.40°N, 117.58°E	900	North China background	39.8±34.0	1035
Xishuangbanna/BNF	21.90°N, 101.27°E	560	Southwestern rain forest	25.0±18.7	707
Yantai/YTZ	36.05°N, 120.27°E	47	East China sea coast city	51.1±36.7	915
Yucheng/YCA	36.95°N, 116.60°E	22	North China country	102.8±61.8	1008
Zangdongnan/ZDN	29.77°N, 94.73°E	2800	Southern Tibet forest	12.3±8.0	475

Table 2 Summary of the concentrations of $PM_{2.5}$ and its components ($\mu g/m^3$) in urban and background sites.

Station	$PM_{2.5}$	OM	EC	NO_3^-	SO_4^{2-}	NH_4^+	MD*	Cl^-	Unaccounted**
Urban sites									
BJC(n=88)	71.7(36.0)	19.1(11.0)	4.1(1.1)	9.3(7.5)	11.9(8.2)	5.3(2.7)	4.7(2.9)	0.7(1.0)	16.5(11.8)
SHC(n=120)	68.4(20.3)	17.1(4.5)	2.0(0.6)	11.9(5.0)	13.6(6.4)	5.8(2.1)			18.1(4.9)
GZC(n=106)	75.3(37.7)	16.7(10.0)	7.1(4.8)	7.2(7.9)	13.1(7.9)	4.8(3.5)	7.3(3.3)	1.0(1.1)	18.1(13.1)
LSZ(n=60)	36.4(18.7)	12.6(1.9)	1.4(0.6)	0.5(0.2)	0.8(0.4)	0.4(0.2)	11.6(12.9)	0.3(0.1)	8.8(7.8)
SYC(n=36)	81.8(55.6)	23.3(22.3)	5.2(3.4)	4.6(4.7)	13.2(10.7)	4.5(2.6)	9.2(5.6)	1.4(1.4)	20.4(15.8)
CQC(n=56)	73.5(30.5)	17.2(8.2)	4.8(1.6)	6.5(6.2)	19.7(9.6)	6.1(2.7)	7.4(3.5)	0.6(0.4)	11.2(6.1)
Background sites									
XLZ(n=42)	42.6(20.1)	12.4(5.1)	1.5(0.7)	3.7(5.0)	8.4(7.0)	3.4(2.2)	5.0(2.7)	0.3(0.3)	7.9(5.6)
LAZ(n=60)	66.3(36.6)	21.7(6.5)	2.9(1.4)	8.7(8.5)	11.2(6.3)	7.3(4.5)	2.0(2.0)	0.6(0.8)	11.9(8.2)
DHM(n=36)	40.1(20.4)	11.6(5.0)	2.0(1.0)	4.5(3.9)	10.1(5.3)	4.0(1.7)	3.8(0.9)	0.5(0.6)	3.6(1.5)
NMT(n=35)	9.5(10.7)	3.4(2.7)	0.2(0.5)	0.1(0.1)	0.4(0.4)	0.4(0.2)	3.9(2.0)	0.1(0.0)	1.1(2.6)
CBM(n=52)	23.3(6.8)	8.9(3.6)	0.9(0.6)	1.1(1.4)	3.3(2.3)	1.8(0.9)	3.7(1.9)	0.2(0.2)	3.5(3.4)
GGM(n=36)	32.2(29.7)	13.1(13.5)	1.1(0.8)	0.4(0.5)	4.7(4.1)	1.7(1.3)	3.2(2.9)	0.4(1.4)	7.7(8.0)

*MD: mineral dust; **Unaccounted: the difference between the $PM_{2.5}$ gravimetric mass and the sum of the PM constituents (OM, EC, SO_4^{2-}, NO_3^-, NH_4^+,Mineral dust and Cl^-).

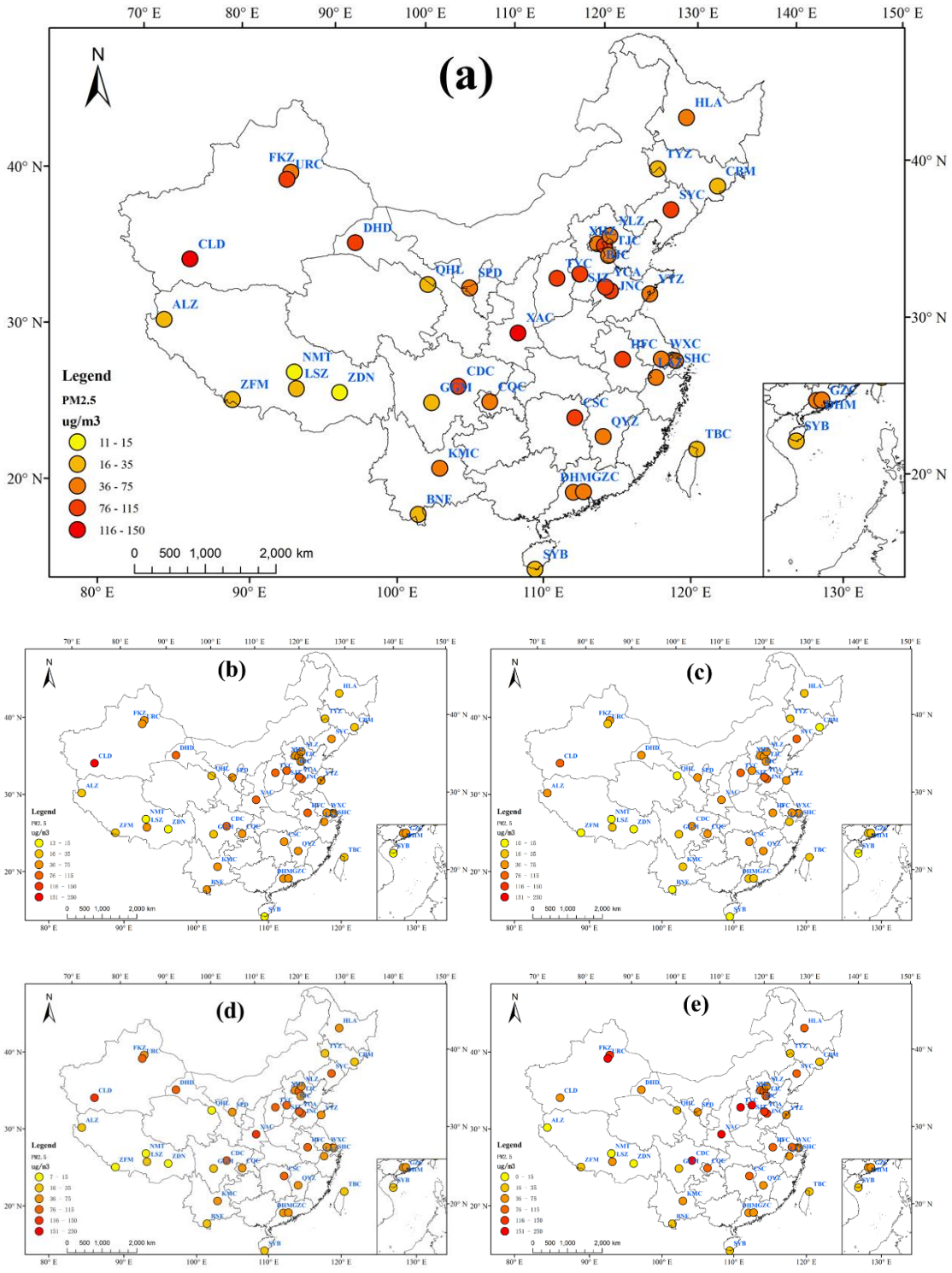

Fig.1. Locations and the averaged $PM_{2.5}$ concentrations of the forty monitor stations during (a) the year of 2012-2014, (b) spring, (c) summer, (d) autumn and (e) winter. The site code related to the observation stations could be found in Table 1.

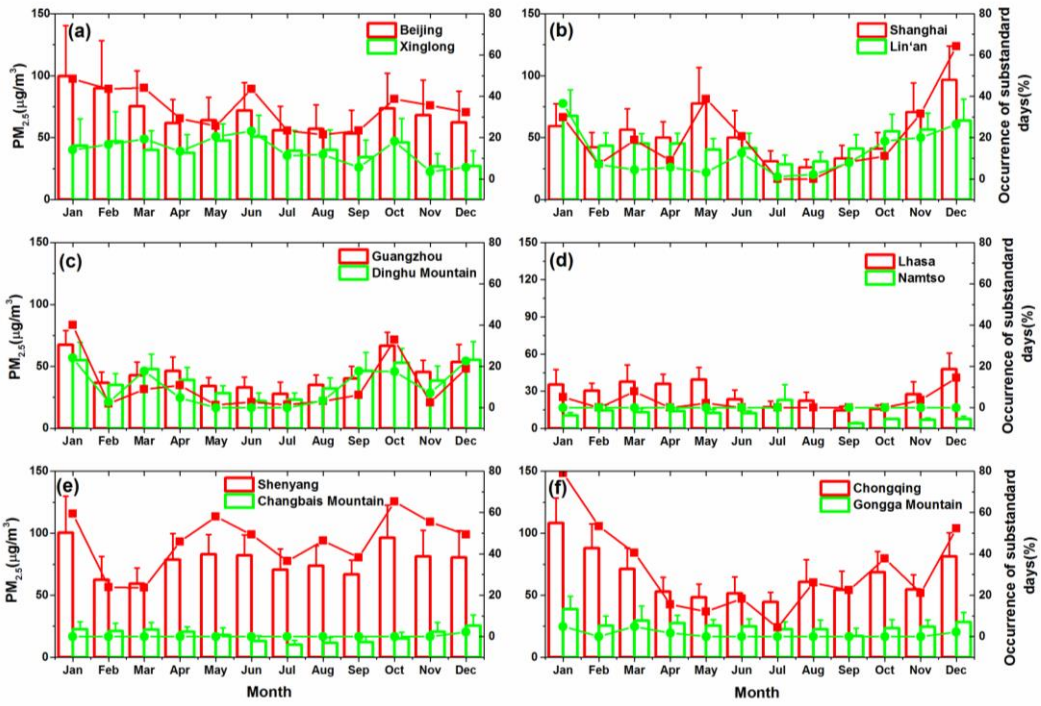

Fig.2. Monthly average $PM_{2.5}$ concentration (histogram, left coordinate) and the occurrence of substandard days in each month (dotted line, right coordinate) at urban and background sites in (a)North China plain, (b)Yangtze River delta, (c) Pearl River delta, (d)Tibetan Autonomous Region , (e) Northeast China Region and (f) Southwestern China Region. The error bars stands for the standard deviation.

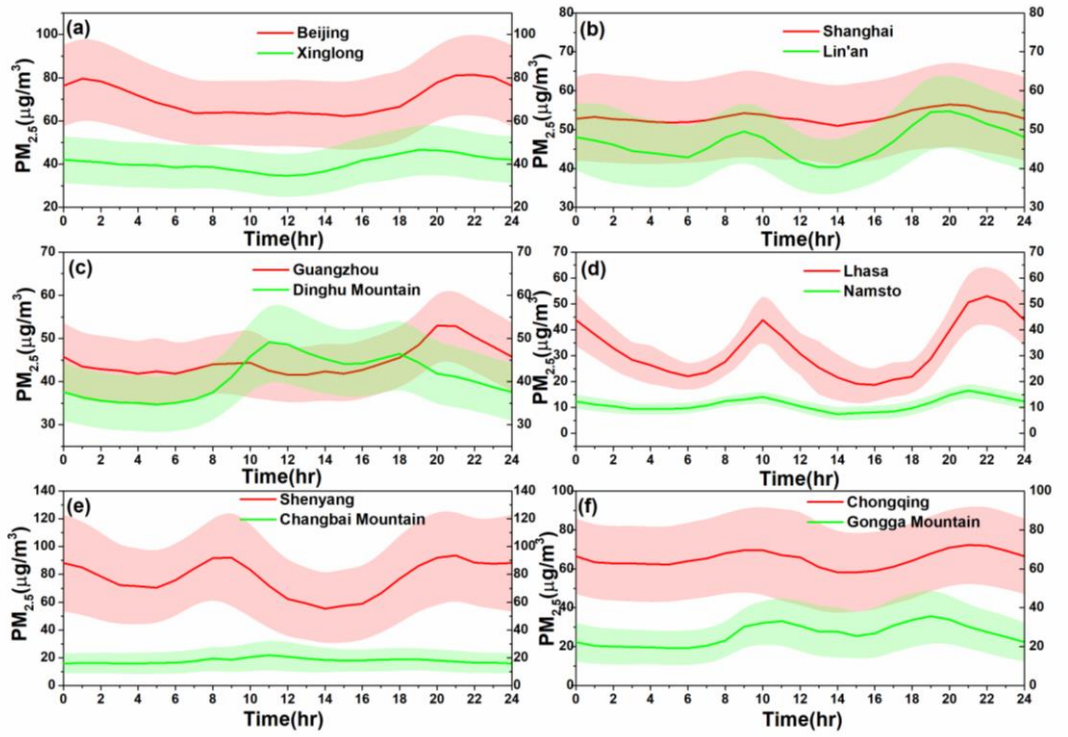

Fig.3 Diurnal cycles of $PM_{2.5}$ at six paired urban and background sites in (a)North China plain, (b)Yangtze River delta, (c) Pearl River delta, (d)Tibetan Autonomous Region, (e) Northeast China Region and (f) Southwestern China Region. Shadow area represent the error bars and stands for one half of the standard deviation.

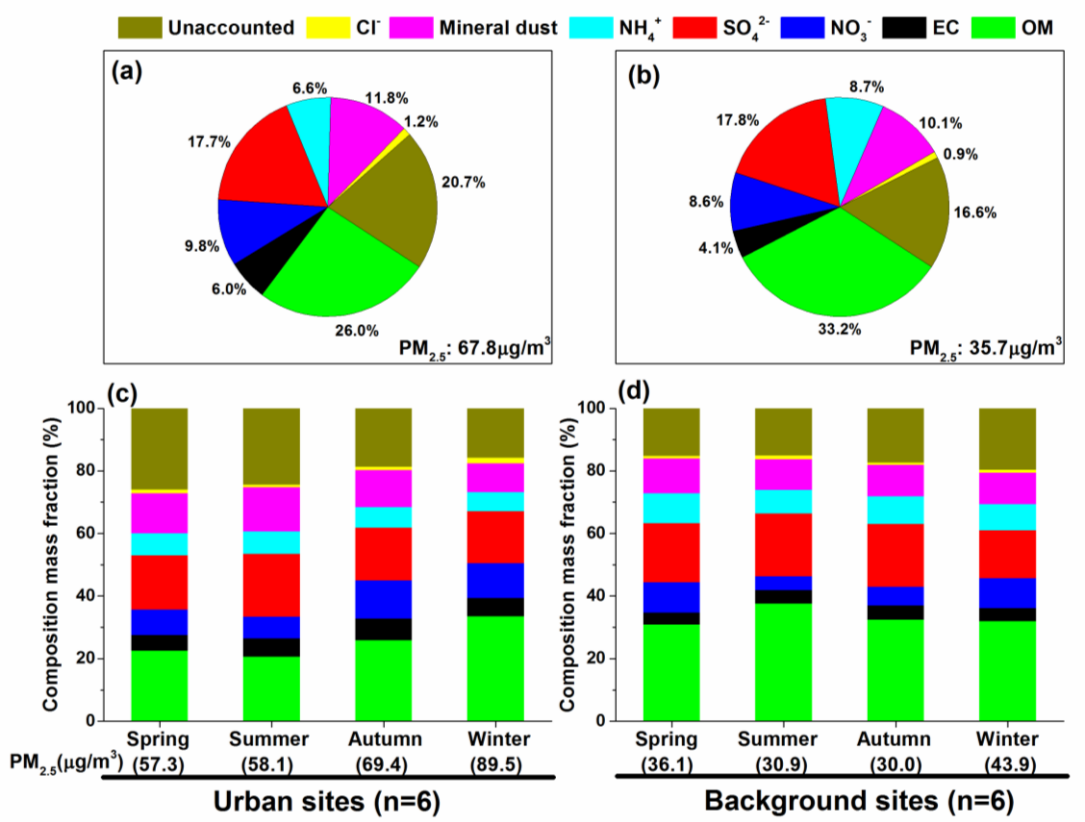

Fig. 4 Average chemical composition and its seasonal variations of $PM_{2.5}$ in (a, c) urban sites and (b, d) background sites. The unaccounted matter refer to the difference between the $PM_{2.5}$ gravimetric mass and the sum of the PM constituents (OM, EC, SO_4^{2-}, NO_3^-, NH_4^+,Mineral dust and Cl^-).

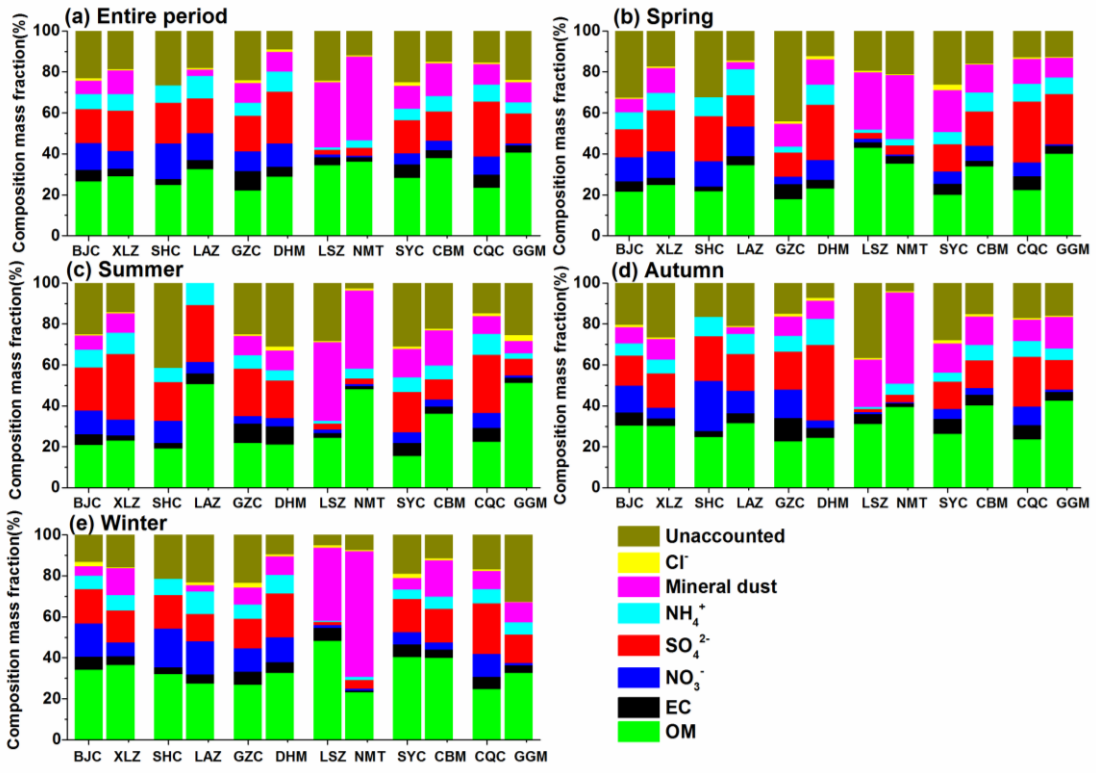

Fig.5 Average chemical composition of $PM_{2.5}$ in individual site during (a) the entire period and (b-e) the different seasons. The unaccounted matter refer to the difference between the $PM_{2.5}$ gravimetric mass and the sum of the PM constituents (OM, EC, SO_4^{2-}, NO_3^-, NH_4^+,Mineral dust and Cl^-). The site code related to the observation stations could be found in Table 1.

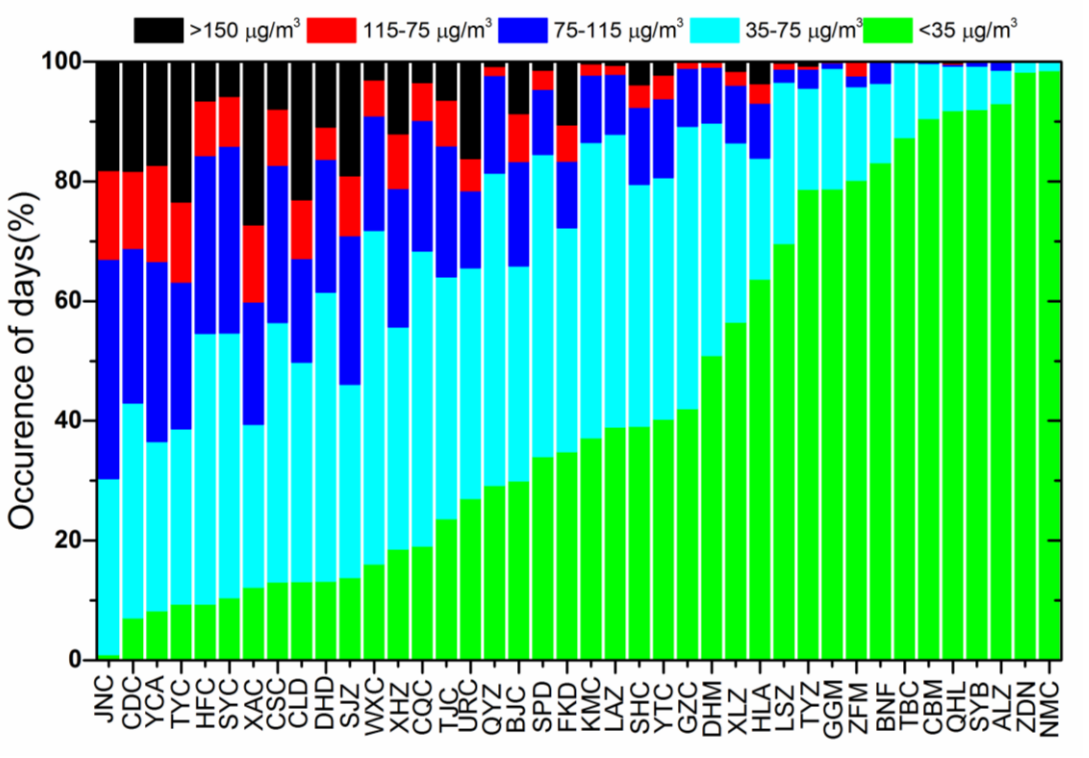

Fig.6 Days separated by the threshold values of the "Ambient Air Quality Standard" (AAQS) (GB3095-2012) of China guideline. The threshold values of 35, 75, 115 and 150μg/m^3 used for the daily concentration ranges are represented as clean (<35μg/m^3), slightly polluted (35-75μg/m^3), moderated polluted (75-115μg/m^3), polluted (115-150μg/m^3) and heavily polluted (>150μg/m^3), which suggested by the guideline of the AAQS. The site code related to the observation stations could be found in Table 1.

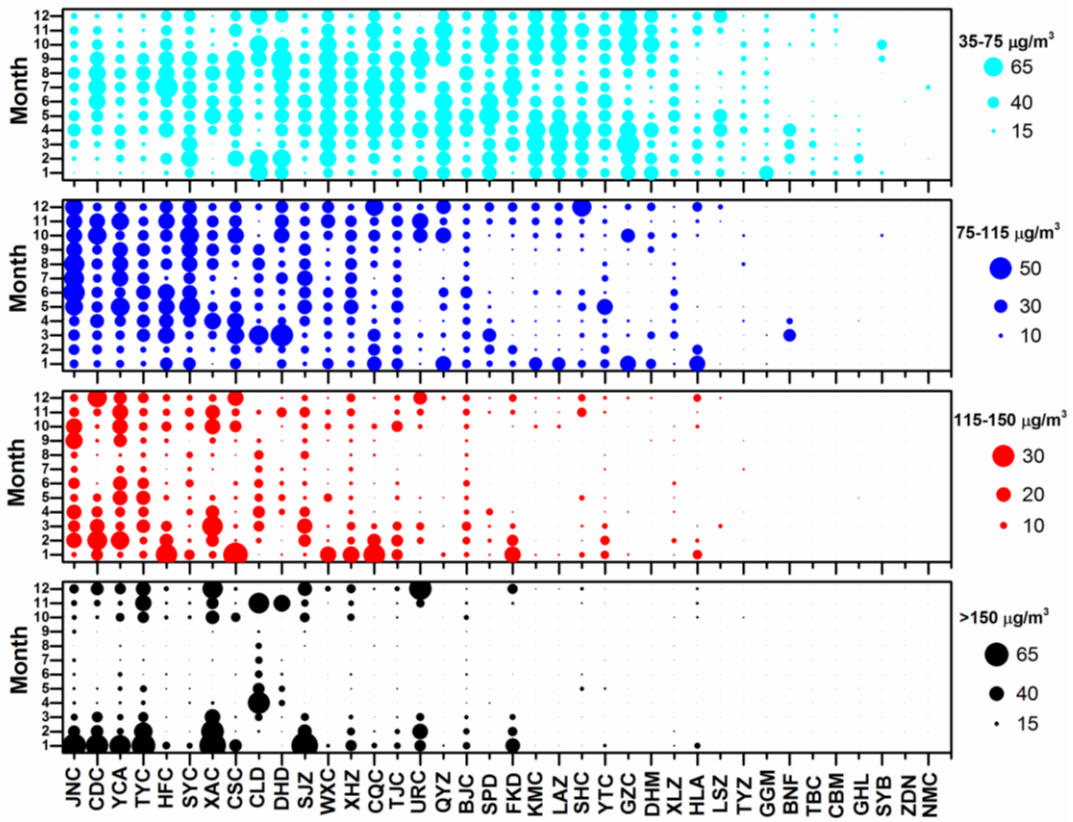

Fig.7 Monthly distribution of the occurrence of the polluted days exceeding the "Ambient Air Quality Standard" (AAQS) (GB3095-2012) of China. The symbol size represents the occurrences of polluted days for the corresponding month. The symbol color represents the different mass range. The sites of Nagri and Mount Everest are excluded because of the small sample size. The site code related to the observation stations could be found in Table 1.

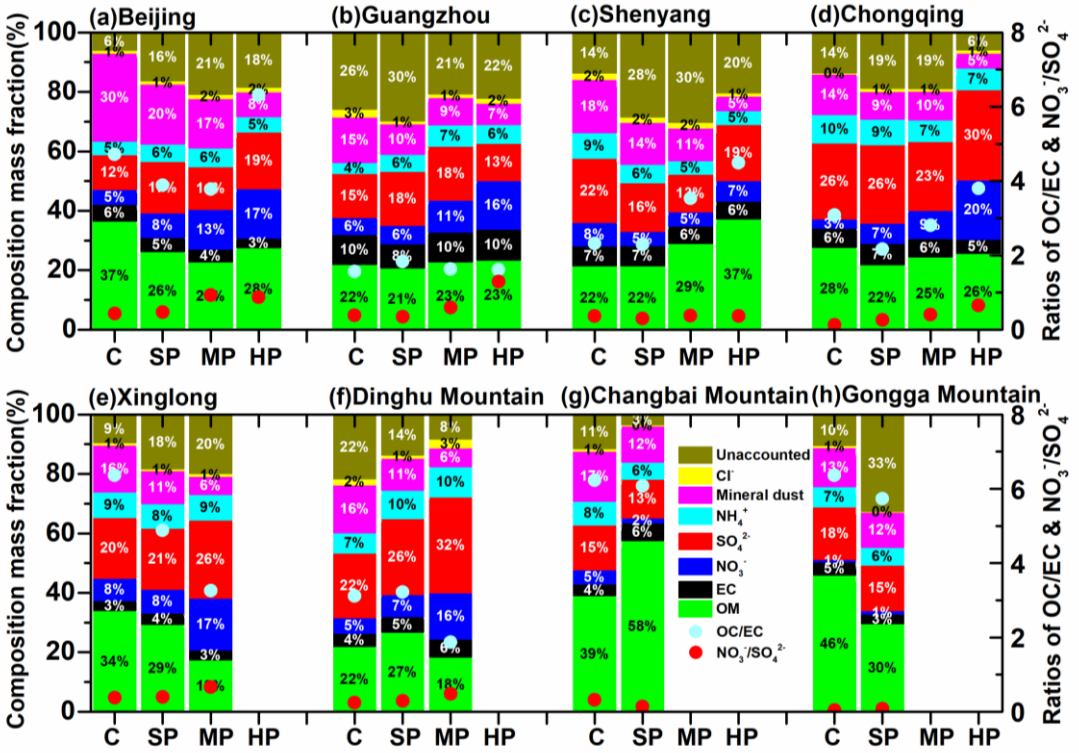

Fig. 8 Average chemical composition of $PM_{2.5}$ and the mass ratio of $[NO_3^-]/[SO_4^{2-}]$ and OC/EC with respect to pollution level. The C, SP, MP and HP is related to clean (daily $PM_{2.5}$ <35 μg/m^3), slightly polluted (35 μg/m^3<daily $PM_{2.5}$ <75 μg/m^3), moderated polluted (75 μg/m^3<daily $PM_{2.5}$ <150 μg/m^3) and heavily polluted (daily $PM_{2.5}$ >150 μg/m^3). The unaccounted matter refer to the difference between the $PM_{2.5}$ gravimetric mass and the sum of the PM constituents (OM, EC, SO_4^{2-}, NO_3^-, NH_4^+,Mineral dust and Cl^-).